Acronym:	**COCKLES**
Title:	Co-Operation for Restoring CocKle SheLlfisheries and its Ecosystem Services in the Atlantic Area
Contract:	EAPA_458/2016

Deliverable 7.2

Identification of protein markers of marteiliosis resistance

February 2021

Lead Partner for Output	Centro de Investigacións Mariñas (CIMA)
Contributors	Asunción Cao, David Iglesias, María J. Carballal, Antonio Villalba
Due date of Output	30/04/2020
Actual submission date	24/02/2021

Dissemination level			
☒	**PU** Public	☐	**PP** Restricted to other programme participants
☐	**RE** Restricted to a group specified by the Consortium	☐	**CO** Confidential, only for members of the Consortium

Acknowledgement

The work described in this report has been funded by the European Commission under the INTERREG-Atlantic Area Programme.

Contents

1. Executive Summary

The cockle fishery of the ria of Arousa collapsed in 2012 due to an unprecedented huge mortality of cockles caused by marteiliosis (infection with the protozoan *Marteilia cochillia*). The disease spread southwards with similar disastrous effects in the rias of Pontevedra and Vigo in 2013 and 2014, respectively. Research for ways to minimise the effect of disease and recover cockle production in the affected Galician rias became peremptory. The project COCKLES assumed as an objective to devise procedures to recover cockle production in marteiliosis-affected areas, using marteiliosis-resistant cockle strains. A first step involved the identification of molecular markers of resistance against *M. cochillia* with which implementing marker-assisted selective breeding programmes envisaged to produce cockle strains resistant to marteiliosis. Two approaches searching for markers of marteiliosis-resistance were accomplished, proteomic and genomic. This report concentrates in the proteomic approach.

The experimental design of the proteomic approach involved comparing the proteome of cockles before being exposed in the field to a marteiliosis outbreak with the proteome of survivors after the outbreak, assuming that some of the proteins differentially expressed in the survivors could be crucial to survive under marteiliosis pressure. Based on the knowledge of marteiliosis dynamics acquired in previous years, field work was performed to expose non-infected cockles to a natural marteiliosis outbreak through two plans. The plan A involved transplanting 2300 adult cockles from a naïve (never affected by marteiliosis) population (a shellfish bed in Noia, ria of Muros-Noia) to a marteiliosis heavily affected area (the shellfish bed of Lombos do Ulla, ria of Arousa) in spring 2018, where they would be affected by a marteiliosis outbreak expected to start in summer 2018. Considering the risk of having insufficient number of survivors due to marteiliosis-caused mortality, another plan (plan B) was implemented, taking advantage of the naturally recruited cockle cohort in the affected shellfish bed of Lombos do Ulla in late spring 2018, before the marteiliosis outbreak and its natural exposure to the marteiliosis outbreak staring in summer 2018. In late spring and early summer 2018, before marteiliosis detection, a sample of transplanted naïve cockles (plan A) and a sample of newly recruited cockles (plan B), respectively, were collected from Lombos do Ulla and processed for proteomic analysis. Additionally, sampling of both the transplanted cockle batch and the

recruited cohort was performed monthly to monitor marteiliosis dynamics; mortality was also estimated monthly. First cases of infection with *M. cochillia* were detected both in transplanted and naturally recruited cockles in late July 2018; the prevalence of marteiliosis increased sharply in the transplanted cockles, reaching 88 % in October, while the prevalence increase more slowly in the naturally recruited cockles and did not overpass 50%. Cumulative mortality of transplanted cockles exceeded 95% in October 2018, which excluded any expectancy of having sufficient survivors after the marteiliosis outbreak; thus, the plan was aborted and discarded. However, cumulative mortality increased more slowly in the naturally recruited cockles and, in July 2019, a sample of the survivors was taken and processed for proteomic analysis. The marteiliosis dynamics recorded within plan B showed a decrease of both marteiliosis prevalence and cumulative mortality compared to records of the period 2012-2016 for cockles recruited in the shellfish bed of Lombos do Ulla; the results suggest that the drops of marteiliosis prevalence and cockle mortality were likely due to an increase of resistance to marteiliosis in the cockle population of the inner side of the ria of Arousa through natural selection rather than to disappearance or lower virulence of *M. cochillia*. An *ad-hoc* experiment was designed to further test this hypothetical gain of marteiliosis resistance in the cockle population of the inner side of the ria of Arousa; the experiment is ongoing within the work package 3 of the project COCKLES.

Proteins were isolated from the soft tissues of the cockles collected before the marteiliosis outbreak (BOB) within plan B as well as from soft tissues of survivors collected after the outbreak (AOB). Their proteomic profiles were compared using a shotgun approach through liquid chromatography (LC) coupled to mass spectrometry (MS). Qualitative comparison allowed the identification of 93 proteins that were found expressed exclusively before the outbreak, 101 proteins exclusively expressed in survivors and 271 proteins in both situations. Quantitative comparison allowed the identification of 45 proteins that were significantly down-regulated and eight significantly up-regulated in the surviving cockles. The eight significantly up-regulated proteins in the survivors have been selected as candidate markers of resistance to marteiliosis. These candidate proteins have to be validated as true markers of marteiliosis resistance through an *ad hoc* experiment.

2. Introduction

The cockle *Cerastoderma edule* fishery has traditionally been the most important shellfishery in terms of biomass on the Galician (NW Spain) coast; the highest cockle production in this region traditionally came from the rias of Arousa and Muros-Noia. An unprecedented huge mortality of cockles, due to **marteiliosis** (infection with the protozoan *Marteilia cochillia*), led to **cockle fishery collapse** in the ria of Arousa (Galicia, NW Spain) in 2012 (Villalba et al 2014) and so did it in the rias of Pontevedra and Vigo in 2013 and 2014, respectively (Iglesias et al., 2015, 2017). From 2012 to 2016, an epidemic pattern was observed, entailing that the newly recruited cockle cohort detected every year in late spring or early summer was affected by marteiliosis that summer or early autumn; marteiliosis prevalence rapidly increased reaching values close to 100 %, causing the extinction of every newly-recruited cockle cohort before reaching market size (Iglesias et al., 2017, 2019). The dramatic losses caused by this highly pathogenic parasite raised the **claims of the Galician shellfish industry for solving the cockle fishery crisis** and led to perform applied research to understand disease dynamics as well as looking for ways to minimise its detrimental effects.

Using therapeutic products to fight cockle marteiliosis in the open sea is wothless, standard vaccination is not an option for molluscs because it does not induce production of antibodies or other molecules conferring long-term protection to previously susceptible individuals, and eradication of marteiliosis from endemic areas does not seem feasible, as it has been proved for other mollusc protozoan-caused endemic diseases, such as flat oyster bonamiosis (Grizel et al., 1987; van Banning, 1991; Lynch et al., 2007). **Producing marteiliosis-resistant cockle strains appears to be a promising approach to overcome this disease** in endemic areas, considering that selective breeding programmes have been successful to increase mollusc resistance against various diseases (Ford & Haskin, 1987; Beattie et al., 1988, Ragone Calvo et al., 2003; Dove et al., 2013; Dégremont et al., 2015a, 2015b, 2015c, 2019, 2020; Smits et al., 2020a), which has led mollusc industry and Administration to opt for this strategy, selective breeding for resistance, to fight a number of mollusc diseases (Frank-Lawale et al., 2014; Lynch et al., 2014; Proestou et al., 2016; Sunila et al., 2016; Casas et al., 2017; Lapègue & Renault, 2018; Cruz et al., 2020).

Bivalve molluscs have an effective innate immune system that acts as the main defence mechanism against pathogens. The innate immune system allows the host to detect a wide variety of pathogens, ranging from viruses to multicellular parasites, providing protection against infection to the host (Hargreaves & Medzhitov, 2005). The innate immune system process of bivalves can be summarized in three main steps: (i) the recognition of molecular motifs associated with microorganisms or endogenous molecules secreted by damaged tissues by soluble compounds and cellular receptors, (ii) the activation of different signalling pathways, (iii) the production of molecular effectors involved in host defence and cellular defence responses (Allam & Raftos, 2015). More or less subtle differences in the mollusc immune response might be the key of the susceptibility or resistance of molluscs to diseases. Understanding the molecular basis of those differences responsible for being susceptible or resistant to a particular disease and identifying molecular markers of resistance should help to find ways to fight mollusc diseases. Recently, much research effort is being focused on the **identification of molecular markers of disease resistance**, through **genomic** (He et al. 2012; Meistertzheim et al., 2014; Nikapitiya et al., 2014; Nie et al., 2015; Wang et al., 2016; Gutiérrez et al., 2018; La Peyre et al. 2019; Vera et al., 2019; de Lorgeril et al., 2020; Farhat et al., 2020; Gutiérrez et al., 2020; Hasanuzzaman et al., 2020; Proestou & Sullivan, 2020) and **proteomic** approaches (Simonian et al., 2009; Fernández Boo et al., 2016; de la Ballina et al., 2018; Vaibhav et al., 2018; Smits et al., 2020b; Leprêtre et al., 2021), that can be used in **marker-assisted selection programmes** in order to increase the efficiency and shorten the process of disease resistance gaining.

Considering the relevance of cockle marteiliosis, at least for Galician cockle beds, the project COCKLES assumed as an objective **to devise procedures to recover cockle production in marteiliosis-affected areas, using marteiliosis-resistant cockle strains.** A step (partial objective, milestone) within this context was **the identification of molecular markers of resistance against *M. cochillia*** with which implementing marker-assisted selective breeding programmes envisaged to produce cockle strains resistant to marteiliosis. Two approaches searching for markers of marteiliosis-resistance were accomplished, proteomic and genomic. **This report concentrates in the proteomic approach**, while the genomic one is addressed in

the deliverable 7.3. The experimental design of the proteomic approach involved comparing the proteome of cockles before being exposed in the field to a marteiliosis outbreak with the proteome of survivors after the outbreak, assuming that some of the proteins differentially expressed in the survivors could be crucial to survive under marteiliosis pressure. A proteomic shotgun procedure allowed finding qualitative and quantitative differences in protein expression and, after statistical analysis and functional characterisation, **eight proteins are proposed as candidates for marteiliosis-resistance markers**. Additionally, relevant information on marteiliosis dynamics suggesting an increase of resistance to marteiliosis by natural selection has been obtained.

3. Materials and methods

3.1. Experimental design

The basic pretention consisted of using a batch of cockles from a single cohort (all them from the same place and the same age) that had not been exposed to *M. cochillia*, taking tissue samples from a number of them to characterise their proteome, exposing the remaining cockles in the field to a marteiliosis outbreak, recovering survivors and taking tissue samples to characterise their proteome and, finally, comparing the proteome of survivors with that of cockles processed before being exposed, looking for proteins with differential expression in the survivors that can be considered as having a role in marteiliosis-resistance. This pretension required taking advantage of a natural marteiliosis outbreak. Our previous research on cockle-marteiliosis dynamics in the period 2012-2016 in a shellfish bed, Lombos do Ulla (42° 37,757´ N, 8° 46,521’ W), located in the inner side of the ria of Arousa, had shown an epidemic annual pattern involving the start (first detection) of marteiliosis outbreak in summer or early autumn affecting the newly recruited cockles, with quick transmission, causing mass mortality and disappearance of the whole recruited cohort by next late winter to early spring, before achieving the minimum market size (Iglesias et al., 2017). This previous information allowed stating **the place, Lombos do Ulla**, and **the period, from late 2018 to spring 2019**,in the experimental design.

What about cockle source? Considering that the digestive gland of the cockle is the organ where *M. cochillia* proliferates and that the cockle immune effector cells, the haemocytes (the main cockle cells responsible for pathogen neutralisation), can be easily isolated from haemolymph samples but not from other tissues, *a priori*, the most appropriate organs/tissues for proteomic comparison, in the context of searching for marteiliosis-resistance markers, would be the digestive gland and the haemolymph. Collecting valid haemolymph samples without contamination from other tissues is only feasible when cockles are longer that 20 mm in length (antero-posterior axis). Cockles longer than 20 mm that had not been exposed to *M. cochillia* were not available at areas heavily affected by marteiliosis (that was the case of Lombos do Ulla) because there, cockles became exposed (and infected) at much shorter size. Therefore, the only source of cockles that had not been exposed to *M. cochillia* and were long-enough (<20 mm) to allow haemolymph sampling would be the marteiliosis free areas. A shellfish bed in Noia (inner side of ria of Muros-Noia, 42° 47'25''N 8° 55'22''W) was chosen for this purpose because our previous thorough monitoring guaranteed no previous exposure of cockles to marteiliosis outbreaks in the area. With those previous considerations, an experiment was designed, involving collecting large adult cockles (recruited the previous year) in the *Marteilia* non-affected bed of Noia in April 2018 and transplanting them into the *Marteilia*-affected bed of Lombos do Ulla, setting them within cages to avoid misidentification with local cockles, and letting them there until the end of the expected marteiliosis outbreak. That was the original plan (**plan A**) of the experimental design. However, this plan A entailed a serious risk. Logistic reasons imposed limits to the number of transplanted cockles, 2300 at most, and, taking into account the expectable high mortality during the marteiliosis outbreak, the probability of having an acceptable number of survivors (at least 30 cockles) after the outbreak would be very low; in other words, the risk of having an insufficient number of survivors, which would impede completing a resolutive proteomic comparison, was very high. Because of this risk, in addition to plan A, another plan (**plan B**) was implemented. In the plan B, the risk of insufficient survivors was extenuated by vastly increasing the initial number of cockles that would be exposed to marteiliosis, namely using the whole natural recruitment available in Lombos do Ulla immediately before the outbreak. A drawback of plan B was that

the small size of cockles before the outbreak impeded collecting haemolymph; thus, the whole soft meat had to be used for the proteomic analysis.

3.2. Implementation of Plan A

A total of 2500 adult cockles were collected from the Noia cockle bed on 16th April 2018 and transported to CIMA, where they were distributed into 4 tanks (135 l volume) with open seawater flow (Fig. 1). Thirty cockles were randomly chosen and processed by histology to characterise the health status and confirm the absence of marteiliosis. Additionally, 2300 cockles were marked by drawing a black circle on their shells with a marker pen and covering it with lacquer (Fig. 2). Once all the cockles were marked, one week after their collection from Noia, they were taken from the tanks to be carried to Lombos do Ulla. Cockle mortality in the tanks was 5% in that week. Being on board above the shellfish bed of Lombos do Ulla, the marked cockles were distributed into 18 plastic boxes (120 cockles per box, around 600 cockles / m^2) partially filled with shellfish bed sediment (Fig. 3). The boxes were covered with a plastic net (10 mm mesh), to avoid predation, and arranged in three frame structures (six boxes in each frame structure); those structures with the boxes were submerged to the bottom, on the shellfish bed, and kept connected with a rope to a buoy (Fig. 4). The six boxes of one of the structures (identified by the buoy colour) had a compartment (delimited with a plastic net) in one corner holding 15 cockles for quick mortality estimation when required (Fig. 3), thus avoiding much disturbance to the remaining cockles in the box. On 8th May, 75 cockles were removed from one of the submerged boxes, taken to the laboratory and processed for proteomic analysis. Each structure with the boxes was raised on board monthly to clean the covering nets from algae and other fouling organisms and mortality was estimated; a sample of 20 cockles was also collected for histopathological analysis. This plan A had to be aborted after the huge mortality of cockles during the marteiliosis outbreak; on 15th October 2018 the estimated cumulative mortality was higher than 95%, thus excluding any expectancy of having sufficient survivors after the outbreak.

Figure 1. Tanks with open seawater flow holding cockles collected from Noia.

Figure 2. Cockles marked with a black circle on their shells.

Figure 3. Left: six plastic boxes filled with shellfish-bed sediment, arranged within a frame structure on board a ship. The marked cockles visible on the sediment had just been set and they would burrow within the sediment once boxes were submerged. Compartments delimited with a

net, envisaged for mortality estimation, are visible in one corner of each box. Right: the six boxes covered with a net to avoid predation.

Figure 4. A frame structure with six boxes in the process of submersion in Lombos do Ulla.

3.3. Implementation of Plan B

As soon as the new recruitment of 2018 was detected in the shellfish bed of Lombos do Ulla, on 16th July 2018, 45 cockles of the newly recruited cohort were collected from the shellfish bed of Lombos de Ulla with a dredge and taken to the laboratory for proteomic analysis. Additionally, 30 more cockles were collected for histopathological analysis. Since then, sampling (collection of 30 cockles) of the shellfish bed was performed monthly up to July 2019; the samples were processed for histopathological analysis in order to detect marteiliosis outbreak and monitor its dynamics in the 2018-recruited cohort. Mortality of that cohort was estimated monthly using plastic boxes filled of sediment as those described in the section 3.2 (Figs. 3 and 4), as follows: on 6th August 2018, 90 cockles were collected from the shellfish bed and distributed into 3 plastic boxes (30 cockles in each box) filled with sediment; the boxes within a frame were deployed on the bottom (Fig. 4). In the next monthly sampling date, the boxes were taken on board and the numbers of live and dead cockles in the boxes were counted; each box was refilled with 30 live cockles and, if needed, with sediment, then deployed again on the shellfish bed. This process was repeated monthly to estimate month mortality rates and cumulative mortality. On 10th July 2019, 45 adult cockles (> 20 mm in length, to guarantee they had been recruited the previous year and, therefore, had been exposed to the

marteiliosis outbreak and survived) were collected from that shellfish bed with a dredge, taken to the laboratory and processed for proteomic analysis.

3.4. Histopathological analysis

The cockles collected from boxes deployed on the shellfish bed (plan A) or directly from the sediment of the shellfish bed (plan B) and taken to the laboratory were kept in a tank with open seawater flow for 24 h to allow the elimination of gut contents. The standard processing involved sucking cockles and taking a transversal section (about 5mm thick) of soft tissues, including gills, visceral mass, mantle and foot, was taken from every cockle. However, as cockles of the two first months within plan B were too tiny, the whole soft tissues from each cockle were processed. The tissues were fixed in Davidson's solution, embedded in paraffin and sectioned (5 µm thick) with a rotary microtome. Sections were stained with Harris' haematoxylin and eosin (Howard et al., 2004). A histological section of each cockle was examined under light microscopy for disease diagnosis, particularly, infection with *M. cochillia*.

3.5. Protein extraction for proteomic analysis

The 75 cockles collected from boxes deployed on the shellfish bed of Lombos do Ulla, within plan A, on 8th May 2018 were brought to the laboratory and kept in tanks with open seawater flow for 24 h to allow the elimination of gut contents. As much haemolymph as possible was withdrawn from the posterior adductor muscle of each cockle, using a 30-gauge needle attached to a 1 ml syringe. Right after extraction, haemolymph samples were kept into ice-cold vials to avoid haemocyte aggregation and degradation. A drop from each haemolymph sample was observed under light microscope to assess quality and to estimate haemocyte viability by using the Trypan blue test. Haemolymph samples contaminated with debris, bacteria, gametes or other tissues were discarded. Once the number of acceptable (clean) haemolymph samples reached 45, no more cockles were processed. Clean haemolymph was frozen, lyophilised and stored at -80°C. Furthermore, small pieces digestive gland from each

cockle were also frozen, lyophilised and stored at -80°C. All these samples have not been analysed because the plan A was discarded, as explained above.

The 45 newly recruited cockles collected from the Shellfish bed in Lombos do Ulla on 16th July 2018, within plan B, were brought to the laboratory and kept in tanks with open seawater flow for 24 h to allow the elimination of gut contents. Their whole soft tissues were frozen, lyophilized and stored at -80 °C until further processing for protein extraction and proteomic analysis. The 45 cockles collected from the same bed on 10th July 2019 within plan B, were equally handled until sucked; in this case, the meat of each cockle was longitudinally separated in two halves, one was processed for histopathological analysis and diagnosis of marteiliosis (see above) and the other half was lyophilised and stored at -80 °C. Before proteomic extraction, the stored lyophilised samples of plan B were thawed and pooled as follows: the materials from 20 (randomly selected) cockles collected before exposure to marteiliosis (July 2018) were used to produce four pools (biological replicates), each pool with the materials deriving from five cockles; regarding the cockles collected after the exposure to marteiliosis (July 2019), the materials of 20 cockles that had been diagnosed as free of serious diseases that could affect their proteomic profile (such as disseminated neoplasia, granulomatosis or infection with trematode sporocysts, haplosporidans or *Marteilia cochillia*) were used to produced four pools (biological replicates), each pool with the materials deriving from five cockles. Pooling of samples reduces biological variation by minimising individual variation and increases statistical performance.

Proteins in each pool were extracted by suspending the lyophilized materials in lysis buffer (7 M urea, 2 M thiourea, 4% 3-[(3-Cholamidopropyl) dimethylammonio]-1-propanesulfonate (CHAPS), 0.2% ampholytes, 100 mM dithiothreitol (DDT) and phenylmethanesulfonyl fluorid (PMSF), a protease inhibitor). Proteins were solubilized for 3h at 4 °C with vigorous shaking, and the mixture centrifuged at 16000xg for 30 min. Proteomic analysis was performed by the proteomic facility at Proteomic Unit of the *Fundación Instituto de Investigaciones Sanitarias* (FIDIS), *Complejo Hospitalario Universitario de Santiago de Compostela*, Spain.

3.6. Protein identification by LC-MS/MS

In order to make global protein identification, an equal amount of protein (100 µg) from each pool (biological replicate) was loaded on a 10% SDS-PAGE gel. The run was stopped as soon as the front had penetrated 3 mm into the resolving gel (Bonzon-Kulichenko et al., 2011; Perez-Hernandez et al., 2013) The protein band was detected by Sypro-Ruby fluorescent staining (Lonza, Switzerland), excised, and processed for in-gel, manual tryptic digestion, as described by Shevchenko et al. (1996). Peptides were extracted by carrying out three 20-min incubations in 40 µL of 60% acetonitrile dissolved in 0.5% HCOOH. The resulting peptide extracts were pooled, concentrated in a SpeedVac, and stored at −20 °C.

3.6.1. Mass spectrometric analysis

A total of 4µl (4 µg) of digested peptides were separated using Reverse Phase Chromatography. Gradient was created using a micro liquid chromatography system (Eksigent Technologies nanoLC 400, SCIEX) coupled to high-speed Triple TOF 6600 mass spectrometer (SCIEX) with a micro flow source. The chosen analytical column was a silica-based reversed phase column Chrom XP C18 150 × 0.30 mm, 3 mm particle size and 120 Å pore size (Eksigent, SCIEX). The trap column was a YMC-TRIART C18 (YMC Technologies, Teknokroma with a 3 mm particle size and 120 Å pore size, switched on-line with the analytical column. The loading pump delivered a solution of 0.1% formic acid in water at 10 µl/min. The micro-pump generated a flow-rate of 5 µl/min and was operated under gradient elution conditions, using 0.1% formic acid in water as mobile phase A, and 0.1% formic acid in acetonitrile as mobile phase B. Peptides were separated using a 90 minutes gradient ranging from 2% to 90% mobile phase B (mobile phase A: 2% acetonitrile, 0.1% formic acid; mobile phase B: 100% acetonitrile, 0.1% formic acid).

Data acquisition was performed in a Triple TOF 6600 System (SCIEX, Foster City, CA) using a Data dependent workflow. Source and interface conditions were the following: ion spray voltage floating (ISVF) 5500 V, curtain gas (CUR) 25, collision energy (CE) 10 and ion source gas

1 (GS1) 25. Instrument was operated with Analyst TF 1.7.1 software (SCIEX, USA). Switching criteria was set to ions greater than mass to charge ratio (m/z) 350 and smaller than m/z 1400 with charge state of 2–5, mass tolerance 250 ppm and an abundance threshold of more than 200 counts (cps). Former target ions were excluded for 15 s. The instrument was automatically calibrated every 4 hours using as external calibrant tryptic peptides from PepCalMix.

After MS/MS analysis, data files were processed using ProteinPilotTM 5.0.1 software from Sciex which uses the algorithm ParagonTM for database search and ProgroupTM for data grouping. Data were searched using a Mollusca Uniprot database. False discovery rate was performed using a non-lineal fitting method displaying only those results that reported a1% Global false discovery rate or better (Shilov et al., 2007).

3.6.2. Protein quantification by SWATH (Sequential Window Acquisition of all Theoretical Mass Spectra)

In order to construct the MS/MS spectral libraries, the peptide solutions were analysed by a shotgun data-dependent acquisition (DDA) approach by micro-LC-MS/MS. To get a good representation of the peptides and proteins present in all samples, pooled vials of samples from each group were prepared using equal mixtures of the original samples. 4 µL (4µg) of each pool was separated into a micro-LC system Ekspert nLC425 (Eksigen, Dublin, CA, USA) using a column Chrom XP C18 150 × 0.30 mm, 3 mm particle size and 120 Å pore size (Eksigent, SCIEX), at a flow rate of 5µl/min. Water and ACN, both containing 0.1% formic acid, were used as solvents A and B, respectively. The gradient run consisted of 5% to 95% B for 30 min, 5 min at 90% B and finally 5 min at 5% B for column equilibration, for a total run time of 40 min. When the peptides eluted, they were directly injected into a hybrid quadrupole-TOF mass spectrometer Triple TOF 6600 (Sciex, Redwood City, CA, USA) operated with a data-dependent acquisition system in positive ion mode. A Micro source (Sciex) was used for the interface between microLC and MS, with an application of 2600 V voltage. The acquisition mode consisted of a 250 ms survey MS scan from 400 to 1250 m/z followed by an MS/MS scan from 100 to 1500 m/z (25 ms acquisition time) of the top 65 precursor ions from the survey scan, for a total cycle time of 2.8 s. The fragmented

precursors were then added to a dynamic exclusion list for 15 s; any singly charged ions were excluded from the MS/MS analysis.

The peptide and protein identifications were performed using Protein Pilot software (version 5.0.1, Sciex) with a Data were searched using a Mollusca Uniprot database, specifying iodoacetamide as Cys alkylation. The false discovery rate (FDR) was set to 1 for both peptides and proteins. The MS/MS spectra of the identified peptides were then used to generate the spectral library for SWATH peak extraction using the add-in for PeakView Software (version 2.2, Sciex) MS/MSALL with SWATH Acquisition MicroApp (version 2.0, Sciex). Peptides with a confidence score above 99% (as obtained from Protein Pilot database search) were included in the spectral library.

SWATH – MS acquisition was performed on a TripleTOF® 6600 LC-MS/MS system (AB SCIEX). Independent samples were analysed using a data-independent acquisition (DIA) method. Each sample (4 µL) was analysed using the LC-MS equipment and LC gradient described above for building the spectral library but instead using the SWATH-MS acquisition method. The method consisted of repeating a cycle that consisted of the acquisition of 65 TOF MS/MS scans (400 to 1500 m/z, high sensitivity mode, 50 ms acquisition time) of overlapping sequential precursor isolation windows of variable width (1 m/z overlap) covering the 400 to 1250 m/z mass range with a previous TOF MS scan (400 to 1500 m/z, 50 ms acquisition time) for each cycle. Total cycle time was 6.3 s. For each sample set, the width of the 65 variable windows was optimized according to the ion density found in the DDA runs using a SWATH variable window calculator worksheet from Sciex.

The targeted data extraction of the fragment ion chromatogram traces from the SWATH runs was performed by PeakView (version 2.2) using the SWATH Acquisition MicroApp (version 2.0). This application processed the data using the spectral library created from the shotgun data. Up to ten peptides per protein and seven fragments per peptide were selected, based on signal intensity; any shared and modified peptides were excluded from the processing. Five minutes windows and 30 ppm widths were used to extract the ion chromatograms; SWATH quantization was attempted for all proteins in the ion library that were identified by ProteinPilot

with an FDR below 1%. The retention times (RT) from the peptides that were selected for each protein were realigned in each run according to the iRT peptides spiked in each sample and eluted along the whole time axis. The extracted ion chromatograms were then generated for each selected fragment ion; the peak areas for the peptides were obtained by summing the peak areas from the corresponding fragment ions. PeakView computed an FDR and a score for each assigned peptide according to the chromatographic and spectra components; only peptides with an FDR below 5% were used for protein quantization. Protein quantization was calculated by adding the peak areas of the corresponding peptides.

The integrated peak areas (processed. mrkvw files from PeakView) were directly exported to the MarkerView software (AB SCIEX) for relative quantitative analysis. The export will generate three files containing quantitative information about individual ions, the summed intensity of different ions for a particular peptide and the summed intensity of different peptides for a particular protein. MarkerView has been used for analysis of SWATH-MS data reported in other proteomics studies (Luo et al., 2017; Meyer & Schilling, 2017; Ortea et al., 2018; Tan & Chung, 2018) because of its data-independent method of quantization. MarkerView uses processing algorithms that accurately find chromatographic and spectral peaks direct from the raw SWATH data. Data alignment by MarkerView compensates for minor variations in both mass and retention time values, ensuring that identical compounds in different samples are accurately compared to one another. To control for possible uneven sample loss across the different samples during the sample preparation process, we performed a global MLR normalization (Most Likely Ratio) (Redestig et al., 2009; Lambert et al., 2014). Unsupervised multivariate statistical analysis using principal component analysis (PCA) was performed to compare the data across the samples. The average MS peak area of each protein was derived from the replicates of the SWATH-MS of each sample followed by Student's *t*-test analysis using the MarkerView software for comparison among the samples based on the averaged area sums of all the transitions derived for each protein. The *t*-test indicated how well each variable distinguishes the two groups, reported as a *p*-value. For each library, its set of differentially expressed proteins (*p*-value <0.05) with a 1.5 fold in- or decrease was selected.

3.7. Functional annotation

Protein sequences were annotated with a blast search in the NCBI (National Centre for Biotechnology Information database) using blastp algorithm in Blast2Go tool (version 5.2.5, http://www.blast2go.com/), employing a threshold *e*-value of $1x10^{5}$. Gene ontology terms were used to group all sequences with the domains of biological process (BP), molecular function (MF) and cellular component (CC).

4. Results and Discussion

4.1. Assessment of marteiliosis outbreak and monitoring of cockle mortality in the shellfish bed of Lombos do Ulla

Histological sections from the monthly samples deriving from plans A and B were examined to detect the occurrence of infection with *M. cochillia* and, thus, to assess the occurrence of a marteiliosis outbreak and to state the right time to select survivors after exposure to marteiliosis in plan B. The temporal variation of the prevalence of marteiliosis and the cumulative mortality corresponding to plans A and B is shown in Fig. 5. Within plan A, using naïve cockles transferred from Noia into Lombos do Ulla, marteiliosis was first detected in July 2018 and increased sharply, reaching 88 % in October. The cumulative mortality of cockles within plan A had overpassed 95% in October 2018, which nullified the expectation of having enough survivors in the next spring, after the outbreak. Therefore, the plan A was aborted and discarded. However, within plan B, using newly recruited cockles in Lombos do Ulla, marteiliosis was also detected in July 2018 but it did not overpass 50% and cumulative mortality increased more slowly than in plan A. In contrast to the marteiliosis temporal pattern recorded in the period 2012-2016 that had been taken into account for the experimental design, after one year of exposure to marteiliosis, the estimated cumulative mortality of the cockle cohort recruited in 2018 was 65% (in June 2019) and marteiliosis was still present (around 30% prevalent). Considering the time limitations of the study, survival for at least one year exposure to marteiliosis was considered long enough for the purposes of the study and survivors were collected in July 2019 for proteomic analysis.

The marked differences in the prevalence of marteiliosis and the cumulative mortality between the naïve cockles transferred from Noia into Lombos do Ulla and the cockles naturally

recruited in Lombos do Ulla together with the decrease of both marteiliosis prevalence and cumulative mortality detected in the 2018 recruited cockles compared to those recruited in the period 2012-2016 (Iglesias et al. 2017) suggest that the resistance to marteiliosis of the cockle population in the inner side of the ria of Arousa is being enhanced by natural selection through the prolonged exposure to this disease (Iglesias et al., 2019). Considering these encouraging results, an *ad-hoc* experiment was designed to further test this hypothetical gain of marteiliosis resistance in the cockle population of the inner side of the ria of Arousa; the experiment is ongoing within the work package 3 of the project COCKLES.

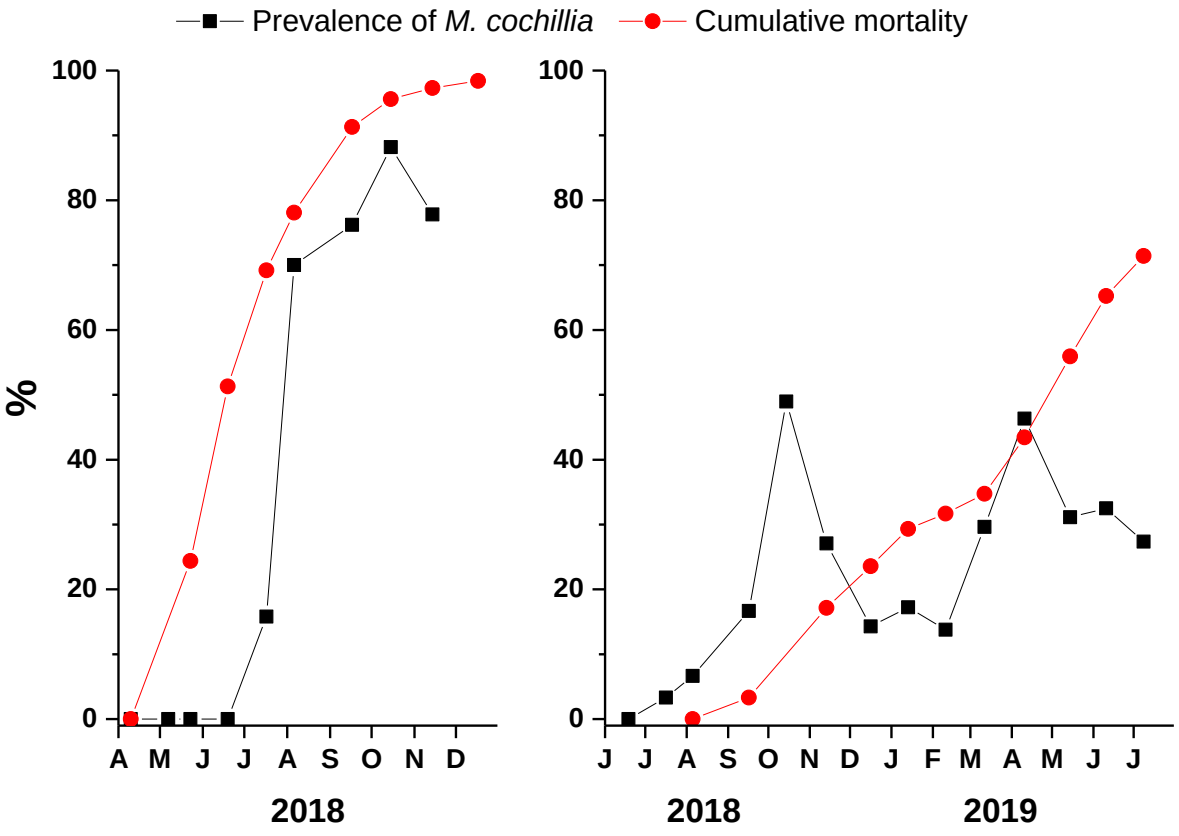

Figure 5. Temporal variation of the prevalence of the infection with *Marteilia cochillia* and the cumulate mortality corresponding to the plans A (left graph) and B (right graph).

4.2. Qualitative analysis of expressed proteins in cockles before and after marteiliosis outbreak.

The proteomic profiles of the cockle soft tissues collected before the outbreak (BOB) were compared with those of the survivors after the outbreak (AOB). The results for qualitative

comparison are shown in Fig. 6. A total of 465 proteins were identified, from which 93 were found expressed exclusively before the outbreak, 101 exclusively in survivors and 271 in both situations.

The annotated proteins were classified according to the Gene Ontology (GO), regarding their allocation in categories of biological process, molecular function and cellular component. The distribution of the proteins exclusive of BOB and those exclusive of AOB in those categories is summarized in Fig. 7. Remarkably, the percentages of proteins associated with catalytic activity and binding was higher in the group of BOB exclusive proteins, while proteins associated with structural molecule activity, response to stimulus and signalling were represented only in the AOB exclusive proteins. The complete list of annotated proteins exclusive of BOF is provided in Table 1 and those exclusive of AOF in Table 2.

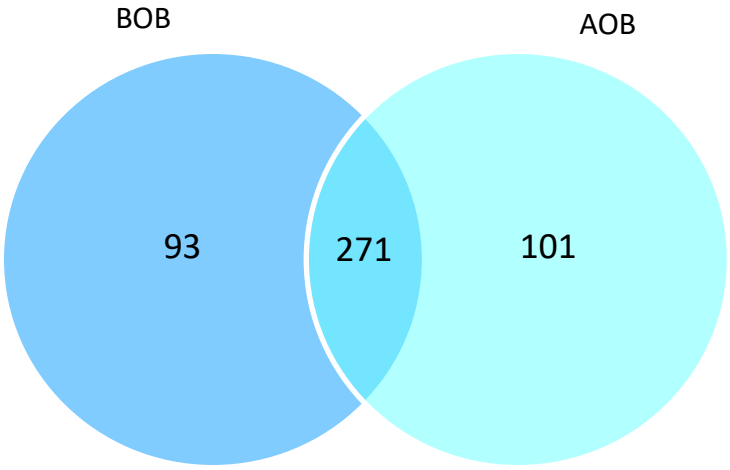

Figure 6. Venn diagram showing the numbers of shared and unique proteins identified in cockles collected before the outbreak (BOB) of marteiliosis and in the survivors collected after the outbreak (AOB).

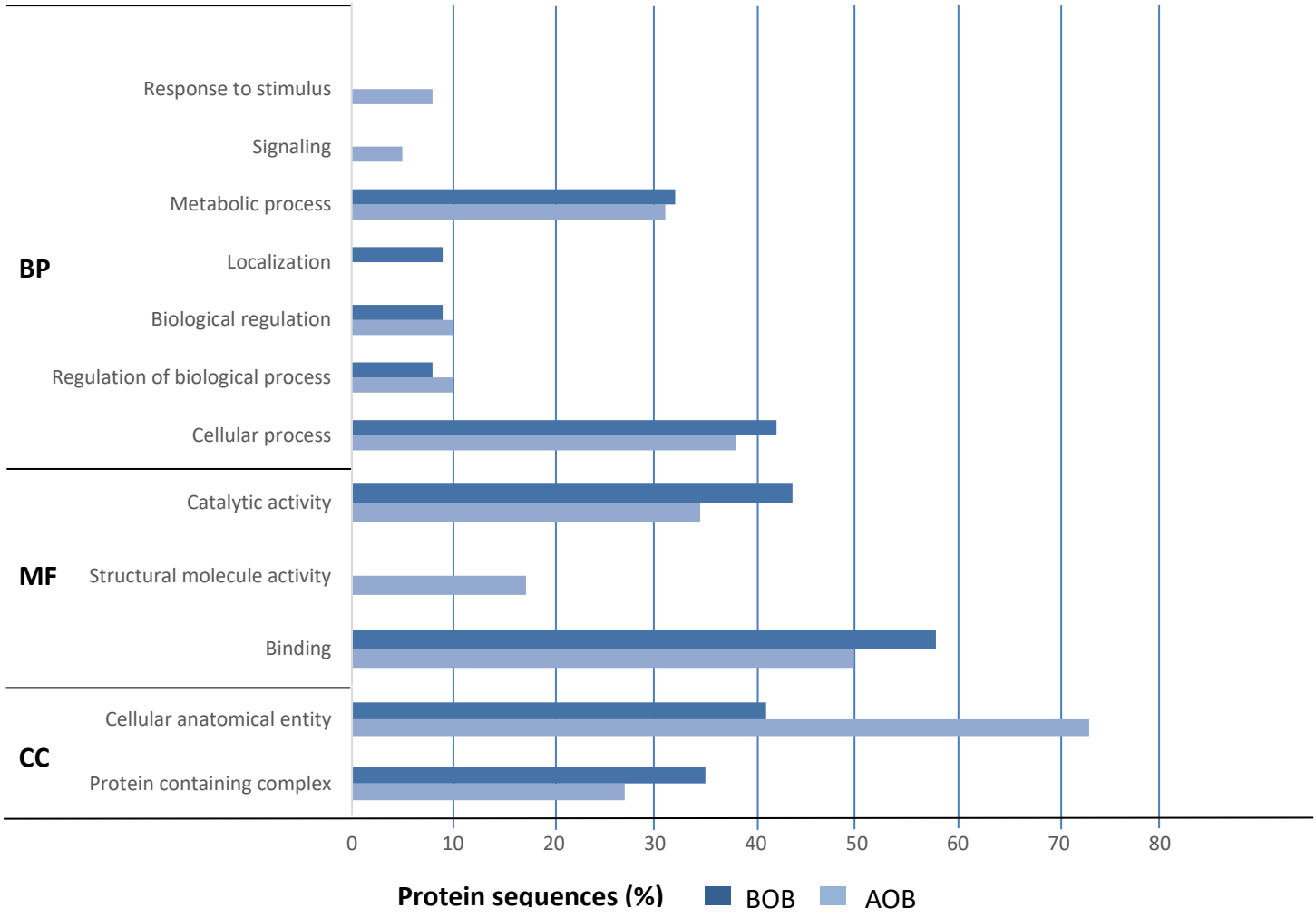

Figure 7. Distribution (percentage) of the proteins representative of cockles collected before the outbreak (BOB) of marteiliosis and those exclusive of survivors after the outbreak (AOB), according Gene Ontology classification for the type of biological process (BP), molecular function (MF) and cellular component (CC).

Table 1. List of identified proteins that were exclusively detected in the soft tissues of surviving cockles collected before the marteiliosis outbreak. SeqName: reference of the sequences identified by MS. Length: Number of amino acids of the sequence. E-Value: is the number of different alignments, with scores equivalent to or better than Score that is expected to occur in a database search by chance. Mean similarity: The percentage of similarity between the protein sequences and the identified protein

SeqName	Description	Length	E-Value	Mean similarity (%)
tr|A0A210PW28|A0A210PW28_MIZYE	10 kDa heat shock protein, mitochondrial-like	105	8.81229E-73	88.68
tr|K1Q1I2|K1Q1I2_CRAGI	26S proteasome regulatory subunit 7	417	0.0	90.13
tr|K1QDM2|K1QDM2_CRAGI	26S proteasome non-ATPase regulatory subunit 2-like	873	0.0	89.64
tr|V4A2A5|V4A2A5_LOTGI	40S ribosomal protein S27-like	84	5.33038E-58	93.65
tr|K1QQ79|K1QQ79_CRAGI	4-aminobutyrate aminotransferase, mitochondrial-like	488	0.0	76.23
tr|K1RBG5|K1RBG5_CRAGI	4-hydroxybutyrate coenzyme A transferase	469	0.0	84.51
tr|Q9XZJ2|Q9XZJ2_CRAGI	heat shock protein 70	659	0.0	96.13
tr|K1R8I8|K1R8I8_CRAGI	dihydrolipoyllysine-residue acetyltransferase component of pyruvate dehydrogenase complex, mitochondrial-like	484	0.0	70.83
tr|K1RBG6|K1RBG6_CRAGI	actin ovestestis isoform	530	0.0	91.73
tr|V4A3I4|V4A3I4_LOTGI	S-adenosylhomocysteine hydrolase-like protein 1 isoform X6	457	0.0	96.4
tr|K1R0Y9|K1R0Y9_CRAGI	ADP,ATP carrier protein 3, mitochondrial-like	306	0.0	91.11
tr|K1RAE9|K1RAE9_CRAGI	ADP-ribosylation factor-like protein 8A	185	2.62528E-138	87.97
tr|A0A210PVE0|A0A210PVE0_MIZYE	alpha-adducin-like isoform X1	824	0.0	95.36
tr|A0A210Q1H1|A0A210Q1H1_MIZYE	sodium bicarbonate cotransporter 3-like isoform X2	1042	0.0	77.5
tr|A0A210R6E5|A0A210R6E5_MIZYE	ankyrin-2-like isoform X16	3209	0.0	85.88
tr|V4A112|V4A112_LOTGI	AP-2 complex subunit alpha-2-like	961	0.0	87.73
tr|A0A0B6ZCF1|A0A0B6ZCF1_9EUPU	actin-related protein 2/3 complex subunit 2-like	318	0.0	88.84
tr|A0A194AL63|A0A194AL63_PINFU	ATP synthase subunit beta, mitochondrial	523	0.0	92.53
tr|K1R5S1|K1R5S1_CRAGI	ATP synthase subunit gamma, mitochondrial-like	211	1.47443E-155	77.67
tr|A0A1S5WH81|A0A1S5WH81_CONMI	V-type proton ATPase subunit B	512	0.0	89.84
tr|K1R185|K1R185_CRAGI	bifunctional 3'-phosphoadenosine 5'-phosphosulfate synthase-like isoform X2	609	0.0	93.67
tr|V4A0Q2|V4A0Q2_LOTGI	programmed cell death 6-interacting protein-like isoform X1	811	0.0	84.63
tr|A0A0L8FKD8|A0A0L8FKD8_OCTBM	protocadherin Fat 4-like	151	3.55619E-105	67.92
tr|A0A0A7RPS6|A0A0A7RPS6_LITLI	calreticulin	408	0.0	90.07
tr|A0A210QYF7|A0A210QYF7_MIZYE	cAMP-dependent protein kinase regulatory subunit isoform X2	371	0.0	94.64

SeqName	Description	Length	E-Value	Mean similarity (%)
tr|V4AGM9|V4AGM9_LOTGI	collagen alpha-2(IV) chain-like	224	2.19658E-158	86.13
tr|V4B153|V4B153_LOTGI	NADH dehydrogenase [ubiquinone] iron-sulfur protein 3, mitochondrial-like	191	1.48963E-141	86.66
tr|A0A210PES1|A0A210PES1_MIZYE	cullin-associated NEDD8-dissociated protein 1-like	1238	0.0	91.84
tr|K1QVP6|K1QVP6_CRAGI	developmentally-regulated GTP-binding protein 1	352	0.0	91.84
tr|A0A210Q8A7|A0A210Q8A7_MIZYE	pyruvate dehydrogenase protein X component, mitochondrial-like	474	0.0	66.59
tr|V3ZEM0|V3ZEM0_LOTGI	dolichyl-diphosphooligosaccharide--protein glycosyltransferase 48 kDa subunit-like	435	0.0	85.57
tr|V3ZSM7|V3ZSM7_LOTGI	integrator complex subunit 1-like	2132	0.0	72.76
tr|K1PAG1|K1PAG1_CRAGI	dynein beta chain, ciliary-like	4464	0.0	85.77
tr|A0A210QI95|A0A210QI95_MIZYE	dynein intermediate chain 2, ciliary-like isoform X4	713	0.0	88.12
tr|A0A210QRY3|A0A210QRY3_MIZYE	endothelial differentiation-related factor 1-like	143	1.80172E-89	81.69
tr|V4AI12|V4AI12_LOTGI	eukaryotic peptide chain release factor subunit 1	441	0.0	96.29
tr|K1P5V7|K1P5V7_CRAGI	eukaryotic translation initiation factor 3 subunit C-like isoform X1	1047	0.0	89.67
tr|K1QCU0|K1QCU0_CRAGI	eukaryotic translation initiation factor 3 subunit G-like	1399	0.0	83.13
tr|A0A210PSK2|A0A210PSK2_MIZYE	far upstream element-binding protein 1-like isoform X1	727	0.0	74.9
tr|K7R6W0|K7R6W0_9BIVA	ferritin	174	6.59025E-130	89.74
tr|A0A2C9JI99|A0A2C9JI99_BIOGL	flotillin-2a-like isoform X2	281	2.92487E-166	90.4
tr|A0A210Q191|A0A210Q191_MIZYE	gelsolin-like protein 2	367	0.0	66.82
tr|V4AI14|V4AI14_LOTGI	glycerol-3-phosphate dehydrogenase [NAD(+)], cytoplasmic-like	351	0.0	84.02
tr|K1QLK8|K1QLK8_CRAGI	GTP-binding protein SAR1-like isoform X1	223	1.65811E-131	93.25
tr|V5KDC4|V5KDC4_9BIVA	heat shock protein 60	159	2.7069E-110	93.71
tr|C8CBM4|C8CBM4_RUDPH	dnaJ homolog subfamily B member 13-like	317	0.0	87.24
tr|A0A210QN27|A0A210QN27_MIZYE	heat shock protein 68-like	646	0.0	92.84
tr|A0A0L8HWE7|A0A0L8HWE7_OCTBM	histone H2B, gonadal-like	91	4.17646E-62	100.0
tr|A0A210QTS2|A0A210QTS2_MIZYE	histone-lysine N-methyltransferase SETD1B-A-like	1713	0.0	76.01
tr|A0A0L8G7T8|A0A0L8G7T8_OCTBM	isocitrate dehydrogenase [NADP] cytoplasmic-like	344	0.0	90.61
tr|A0A0B6ZJS1|A0A0B6ZJS1_9EUPU	60S ribosomal protein L27-like	104	3.11325E-44	93.35
tr|K1PU26|K1PU26_CRAGI	cytosolic malate dehydrogenase	331	0.0	86.27
tr|K1R4Z3|K1R4Z3_CRAGI	malate dehydrogenase, mitochondrial-like	280	0.0	86.63
tr|A0A2C9JFH7|A0A2C9JFH7_BIOGL	tolloid-like protein 1	970	0.0	76.45
tr|A0A0L8IE73|A0A0L8IE73_OCTBM	bromodomain-containing protein DDB_G0280777-like	379	0.0	65.67

SeqName	Description	Length	E-Value	Mean similarity (%)
tr|Q9NDL1|Q9NDL1_MIZYE	myosin heavy chain, non-muscle-like isoform X1	1154	0.0	92.76
tr|M5AJN5|M5AJN5_PINFU	myosin heavy chain, striated muscle-like isoform X5	325	0.0	87.03
tr|A0A0B7BLW1|A0A0B7BLW1_9EUPU	cytoplasmic dynein 1 heavy chain 1-like	632	0.0	93.14
tr|A0A210QYJ6|A0A210QYJ6_MIZYE	NAD(P) transhydrogenase, mitochondrial-like	1069	0.0	86.45
tr|V4ALI7|V4ALI7_LOTGI	NADH dehydrogenase [ubiquinone] flavoprotein 1, mitochondrial-like	429	0.0	89.36
tr|A1ILZ8|A1ILZ8_MIZYE	myosin heavy chain, non-muscle-like isoform X1	883	0.0	93.49
tr|V4AGY6|V4AGY6_LOTGI	nucleolar protein 10-like	686	0.0	73.49
tr|V4BHV5|V4BHV5_LOTGI	oxysterol-binding protein-related protein 9-like	729	0.0	85.31
tr|K1PGP0|K1PGP0_CRAGI	PDZ domain-containing protein GIPC1-like	348	0.0	85.97
tr|K1Q615|K1Q615_CRAGI	peroxiredoxin-like isoform X4	251	2.54084E-134	80.56
tr|A0A0B6Y734|A0A0B6Y734_9EUPU	flotillin-2a-like isoform X2	449	0.0	89.86
tr|A0A2C9JNY6|A0A2C9JNY6_BIOGL	arginine kinase	223	6.47306E-168	86.4
tr|K1RHB3|K1RHB3_CRAGI	phosphoenolpyruvate phosphomutase	326	0.0	91.73
tr|B7P030|B7P030_9BIVA	ATP-dependent RNA helicase DDX3X-like isoform X2	760	0.0	89.97
tr|C7EAA2|C7EAA2_HALAI	ATP-dependent RNA helicase DDX3X-like isoform X3	775	0.0	83.17
tr|A0A194AJE0|A0A194AJE0_PINFU	filamin-A isoform X6	472	0.0	91.47
tr|K1QI11|K1QI11_CRAGI	pyruvate dehydrogenase E1 component subunit alpha, mitochondrial-like	447	0.0	81.39
tr|A0A2C9JRD0|A0A2C9JRD0_BIOGL	pyruvate dehydrogenase E1 component subunit beta, mitochondrial-like	372	0.0	72.69
tr|A0A0L8FS70|A0A0L8FS70_OCTBM	rab proteins geranylgeranyltransferase component A 2-like isoform X2	646	0.0	64.42
tr|K1QY04|K1QY04_CRAGI	radial spoke head protein 3 homolog	398	0.0	90.53
tr|A0A210R2A8|A0A210R2A8_MIZYE	prolyl 4-hydroxylase subunit alpha-1-like isoform X2	344	0.0	72.97
tr|Q8ITC2|Q8ITC2_ARGIR	60S ribosomal protein L11-like	167	1.34783E-122	92.65
tr|A0A0L8FF63|A0A0L8FF63_OCTBM	60S ribosomal protein L30-like	116	1.84649E-82	91.47
tr|K1QPK0|K1QPK0_CRAGI	RNA-binding protein Nova-1-like isoform X3	561	0.0	90.92
tr|K1PY30|K1PY30_CRAGI	septin-2 isoform X3	661	0.0	92.34
tr|K1QVD0|K1QVD0_CRAGI	small ribonucleoprotein particle protein SmD3	131	1.53485E-78	85.0
tr|K1QFR9|K1QFR9_CRAGI	spectrin beta chain-like	2419	0.0	91.86
tr|K1QSE6|K1QSE6_CRAGI	mitochondria-eating protein-like isoform X1	594	0.0	87.68
tr|V3ZN51|V3ZN51_LOTGI	staphylococcal nuclease domain-containing protein 1-like	894	0.0	75.23
tr|K1RLC5|K1RLC5_CRAGI	T-complex protein 1 subunit epsilon-like	678	0.0	86.29
tr|K1PXN5|K1PXN5_CRAGI	T-complex protein 1 subunit zeta-like	531	0.0	85.45

SeqName	Description	Length	E-Value	Mean similarity (%)
tr|K1RG91|K1RG91_CRAGI	transgelin-3-like isoform X2	197	3.01963E-102	73.77
tr|V4AWY5|V4AWY5_LOTGI	2-oxoglutarate dehydrogenase, mitochondrial-like isoform X1	947	0.0	75.47
tr|A0A210Q789|A0A210Q789_MIZYE	tripartite motif-containing protein 59-like	509	0.0	61.96
tr|V4B045|V4B045_LOTGI	tubulin beta chain-like	207	3.88717E-143	80.2
tr|A0A210PT48|A0A210PT48_MIZYE	vacuolar protein sorting-associated protein 13A-like isoform X6	3822	0.0	96.47
tr|V3Z9K5|V3Z9K5_LOTGI	dynein intermediate chain 2, ciliary isoform X3	684	0.0	85.8
tr|K1PBK4|K1PBK4_CRAGI	IgGFc-binding protein-like	284	0.0	53.06

Table 2. List of identified proteins that were exclusively detected in the soft tissues of surviving cockles collected after the marteiliosis outbreak. SeqName: reference of the sequences identified by MS. Length: Number of amino acids of the sequence. E-Value: is the number of different alignments, with scores equivalent to or better than Score that is expected to occur in a database search by chance. Mean similarity: The percentage of similarity between the protein sequences and the identified protein

SeqName	Description	Length	E-Value	Mean similarity (%)
tr|K1R5F2|K1R5F2_CRAGI	14-3-3 protein epsilon-like	256	5.87064E-176	86.57
tr|A0A0A7DR29|A0A0A7DR29_9BIVA	peroxisomal multifunctional enzyme type 2-like	132	2.01199E-94	88.98
tr|G8XVB1|G8XVB1_CRAVI	elongation factor-1a	95	3.36066E-63	96.57
tr|A0A210QX92|A0A210QX92_MIZYE	26S proteasome regulatory subunit 10B	391	0.0	93.5
tr|U5IA39|U5IA39_9BIVA	enoyl-CoA hydratase, mitochondrial-like	39	4.31321E-21	92.3
tr|A0A0L8GT57|A0A0L8GT57_OCTBM	26S proteasome non-ATPase regulatory subunit 1-like	996	0.0	88.53
tr|K1PCS4|K1PCS4_CRAGI	eukaryotic translation initiation factor 2 subunit 3, Y-linked	473	0.0	80.32
tr|V4AR50|V4AR50_LOTGI	26S proteasome non-ATPase regulatory subunit 2-like	905	0.0	88.84
tr|K1RCW5|K1RCW5_CRAGI	eukaryotic translation initiation factor 4 gamma 2	1538	0.0	82.97
tr|V3Z447|V3Z447_LOTGI	dihydrolipoyllysine-residue succinyltransferase component of isoform X1	190	8.67434E-138	83.93
tr|Q963E9|Q963E9_BIOGL	2-oxoglutarate dehydrogenase complex, mitochondrial-like	587	0.0	88.96
tr|V4AS57|V4AS57_LOTGI	radixin-like	132	2.36668E-70	86.97
tr|V4B765|V4B765_LOTGI	40S ribosomal protein S25-like	291	0.0	85.81
tr|A0A0L8HXQ8|A0A0L8HXQ8_OCTBM	F-actin-capping protein subunit alpha-like	118	5.80645E-59	96.12
tr|A0A0K0YAX9|A0A0K0YAX9_MYTCO	40S ribosomal protein S26	2416	0.0	77.24
tr|K7R9T1|K7R9T1_9BIVA	filamin-A-like isoform X1	113	9.667E-78	93.96
tr|O9NL94|O9NL94_OCTVU	40S ribosomal protein S3	354	0.0	89.58
tr|A0A210Q4X9|A0A210Q4X9_MIZYE	guanine nucleotide-binding protein G(i) subunit alpha	225	0.0	95.01
tr|A0A210Q2D6|A0A210Q2D6_MIZYE	40S ribosomal protein S3a	670	0.0	80.79
tr|A0A0B6ZHC5|A0A0B6ZHC5_9EUPU	galactocerebrosidase-like isoform X1	211	4.18057E-97	77.06
tr|V9PAK4|V9PAK4_9BIVA	40S ribosomal protein S8-like	293	0.0	85.6
tr|A0A194AQZ8|A0A194AQZ8_PINFU	glutathione reductase, mitochondrial-like	212	1.03394E-128	88.18
tr|T1RK12|T1RK12_HALDI	40S ribosomal protein S8-like	184	5.45047E-108	95.03
tr|B3TK58|B3TK58_HALDV	GTPase HRas	257	0.0	87.81
tr|V3YXK1|V3YXK1_LOTGI	60S acidic ribosomal protein P0-like	446	0.0	71.39
tr|K1RGT9|K1RGT9_CRAGI	deoxynucleoside triphosphate triphosphohydrolase SAMHD1-like isoform X1	313	5.23694E-147	85.35
tr|K1RCB8|K1RCB8_CRAGI	60S ribosomal protein L13a-like	484	0.0	73.36
tr|A0A0M6ZAE3|A0A0M6ZAE3_9BIVA	heat shock protein 12A-like	653	0.0	92.03
tr|A0A210QR10|A0A210QR10_MIZYE	60S ribosomal protein L27-like	173	4.35095E-116	91.42
tr|A0A210Q2T9|A0A210Q2T9_MIZYE	alpha-crystallin A chain-like	334	7.24119E-134	93.35
tr|A0A210QXT4|A0A210QXT4_MIZYE	heterogeneous nuclear ribonucleoprotein A/B-like	428	0.0	96.53
tr|V4AG94|V4AG94_LOTGI	histone-binding protein RBBP4 isoform X2	361	0.0	88.7
tr|A0A210R2R0|A0A210R2R0_MIZYE	vacuolar proton pump subunit B 1-like isoform X1	338	0.0	98.87
tr|C8CBP0|C8CBP0_RUDPH	mitochondrial-like actin	185	4.30173E-138	78.18
tr|A0A288XNJ2|A0A288XNJ2_9MOLL	lysozyme	182	4.90819E-133	90.52
tr|K1QXI5|K1QXI5_CRAGI	ADP-ribosylation factor 1-like 2	398	0.0	75.18
tr|V3ZUY9|V3ZUY9_LOTGI	major egg antigen-like	1004	0.0	71.84
tr|K1QJL6|K1QJL6_CRAGI	lysosomal alpha-mannosidase-like	345	0.0	88.61
tr|A0A210QIF0|A0A210QIF0_MIZYE	microtubule-associated protein RP/EB family member 1-like isoform X3	301	0.0	87.72
tr|V9P9M1|V9P9M1_MYTGA	actin-related protein 2/3 complex subunit 2-like	353	0.0	89.88
tr|A0A0B7A9H6|A0A0B7A9H6_9EUPU	p38 MAP kinase	487	0.0	73.09
tr|A0A210PQI0|A0A210PQI0_MIZYE	phenylalanine--tRNA ligase beta subunit-like	726	0.0	86.47
tr|V4BWJ9|V4BWJ9_LOTGI	NADH-ubiquinone oxidoreductase 75 kDa subunit, mitochondrial-like	149	2.15699E-104	99.19
tr|A0A2C9HTA1|A0A2C9HTA1_BIOGL	calmodulin	1295	0.0	75.48
tr|A0A269MVC2|A0A269MVC2_BIOGL	neurofilament medium polypeptide-like linear gramicidin synthase subunit D-like	226	0.0	93.19
tr|A0A210QEM2|A0A210QEM2_MIZYE	26S proteasome non-ATPase regulatory subunit 11-like	82	2.10328E-44	75.33
tr|V4BDM6|V4BDM6_LOTGI	eccE3 homolog	101	2.01185E-72	68.41
tr|K1PIB7|K1PIB7_CRAGI	ester family protein ABHD6-like 1 isoform X1	743	0.0	76.93
tr|K1RJ70|K1RJ70_CRAGI	cystatin B	528	0.0	88.25
tr|V4AG32|V4AG32_LOTGI	cytosolic non-specific dipeptidase-like	145	3.32049E-95	83.9
tr|V3ZXA6|V3ZXA6_LOTGI	disabled homolog 1-like isoform X1	723	0.0	78.91
tr|A0A140H126|A0A140H126_MYTGA	DNA replication licensing factor mcm7-like	874	0.0	83.34
tr|V4A7R8|V4A7R8_LOTGI	piwi-like protein 1	195	1.56379E-144	80.2
tr|A0A210PQP0|A0A210PQP0_MIZYE	cilia- and flagella-associated protein 20 profilin-like	140	4.93181E-103	74.84
tr|V4A7Q8|V4A7Q8_LOTGI	dynein light chain roadblock-type 2	96	2.01516E-67	89.06
tr|A0A1P8NCJ9|A0A1P8NCJ9_SEPJA	prohibitin 2	298	0.0	85.08

tr|H8XWJ5|H8XWJ5_9MOLL	prohibitin-like	273	0.0	85.66
tr|A0A210QQG9|A0A210QQG9_MIZYE	prominin-1-A-like isoform X1	979	0.0	74.62
tr|A0A2C9K736|A0A2C9K736_BIOGL	proteasome subunit alpha type-4-like	242	9.51585E-161	79.91
tr|A0A194AN82|A0A194AN82_PINFU	putative aminopeptidase W07G4.4	434	0.0	80.38
tr|L8B2J6|L8B2J6_PINFU	60S ribosomal protein L32-like	134	9.69772E-86	91.4
tr|K1Q7K0|K1Q7K0_CRAGI	probable serine carboxypeptidase CPVL	511	0.0	69.35

SeqName	Description	Length	E-Value	Mean similarity (%)
tr|A0A194AK23|A0A194AK23_PINFU	elongin-C	118	2.26331E-82	96.66
tr|B6RB23|B6RB23_HALDI	ras-related protein Rab-1A	205	1.16876E-153	94.58
tr|K1QQV9|K1QQV9_CRAGI	TPR and ankyrin repeat-containing protein 1-like isoform X1	1201	0.0	61.48
tr|K1QE29|K1QE29_CRAGI	myeloid differentiation primary response protein MyD88-like	644	0.0	58.65
tr|A0A0N9HJP7|A0A0N9HJP7_9BIVA	ras-related C3 botulinum toxin substrate 1	192	2.27452E-121	93.84
tr|A0A0B6Z6I5|A0A0B6Z6I5_9EUPU	ribosomal protein L10a	225	4.82406E-134	90.44
tr|J9Q5H7|J9Q5H7_OSTED	60S ribosomal protein L15-like	204	5.89115E-136	89.65
tr|Q8MUE4|Q8MUE4_9BIVA	60S ribosomal protein L44	106	6.33338E-51	93.96
tr|Q8I9M2|Q8I9M2_9BIVA	40S ribosomal protein S14	70	1.11378E-46	98.08
tr|Q8MUE5|Q8MUE5_9BIVA	40S ribosomal protein S20	117	1.18098E-80	96.2
tr|A0A2C9K6D8|A0A2C9K6D8_BIOGL	40S ribosomal protein S11-like	158	5.71847E-106	90.81
tr|K1QMH5|K1QMH5_CRAGI	suppressor of tumorigenicity 14 protein homolog	688	0.0	67.53
tr|V3ZFZ4|V3ZFZ4_LOTGI	small nuclear ribonucleoprotein Sm D2	120	8.80695E-71	93.75
tr|V4C871|V4C871_LOTGI	small ribonucleoprotein particle protein SmD3	127	5.44323E-59	86.48
tr|A0A0A7DR34|A0A0A7DR34_9BIVA	spectrin alpha chain	175	1.12939E-123	95.4
tr|A0A210Q1Q2|A0A210Q1Q2_MIZYE	spliceosome RNA helicase DDX39B	428	0.0	93.55
tr|V4C2C8|V4C2C8_LOTGI	succinate dehydrogenase [ubiquinone] iron-sulfur subunit, mitochondrial-like	265	0.0	87.32
tr|V4ATV5|V4ATV5_LOTGI	T-complex protein 1 subunit eta-like	541	0.0	80.32
tr|A0A2C9M893|A0A2C9M893_BIOGL	tektin-3-like isoform X1	466	0.0	93.39
tr|A0A0U3DY62|A0A0U3DY62_MACCH	thioredoxin peroxidase	224	2.25667E-162	87.59
tr|B1N693|B1N693_HALDI	peroxiredoxin 4 precursor	251	0.0	88.91
tr|A0A0L8I3B2|A0A0L8I3B2_OCTBM	cullin-associated NEDD8-dissociated protein 1-like	1236	0.0	88.99
tr|A0A077H0P3|A0A077H0P3_MYTTR	transcription factor BTF3 homolog 4-like	176	6.8716E-87	88.36
tr|K1R3T3|K1R3T3_CRAGI	transcription factor BTF3 homolog 4-like	170	1.7174E-99	89.61
tr|A0A0B6XYR0|A0A0B6XYR0_9EUPU	transketolase-like isoform X1	625	0.0	85.57
tr|A0A210QTH7|A0A210QTH7_MIZYE	trifunctional enzyme subunit beta, mitochondrial-like	469	0.0	70.64
sp|Q95WY0|TPM03_CRAGI	tropomyosin isoform X5	233	1.25324E-127	96.14
tr|G3ET94|G3ET94_9BIVA	tubulin beta chain-like	376	0.0	96.37
tr|K1QFF0|K1QFF0_CRAGI	vacuolar protein sorting-associated protein 35-like	797	0.0	92.78
tr|A0A210Q386|A0A210Q386_MIZYE	WD repeat-containing protein 5B	415	0.0	89.46

4.3. Quantitative comparison by SWATCH-MS analysis of protein expression in cockles collected before and after the marteiliosis outbreak.

A comparative quantitative analysis of the protein expression in the cockles collected before and after the marteiliosis outbreak was performed. For optimum display and visualization, a Volcano plot showing the log2 of the fold-change for each protein as a function of the p-value is provided in Fig. 8. Proteins with a p-value< 0.05 and a large fold-change >1.5 were considered significantly regulated. With these criteria, 53 protein appeared differentially expressed in the cockles collected after outbreak of *M. cochillia*, 45 proteins were found down-regulated and 8 up-regulated. The intensity of the expression changes of the differentially expressed proteins are shown as a heat map in Fig. 9.

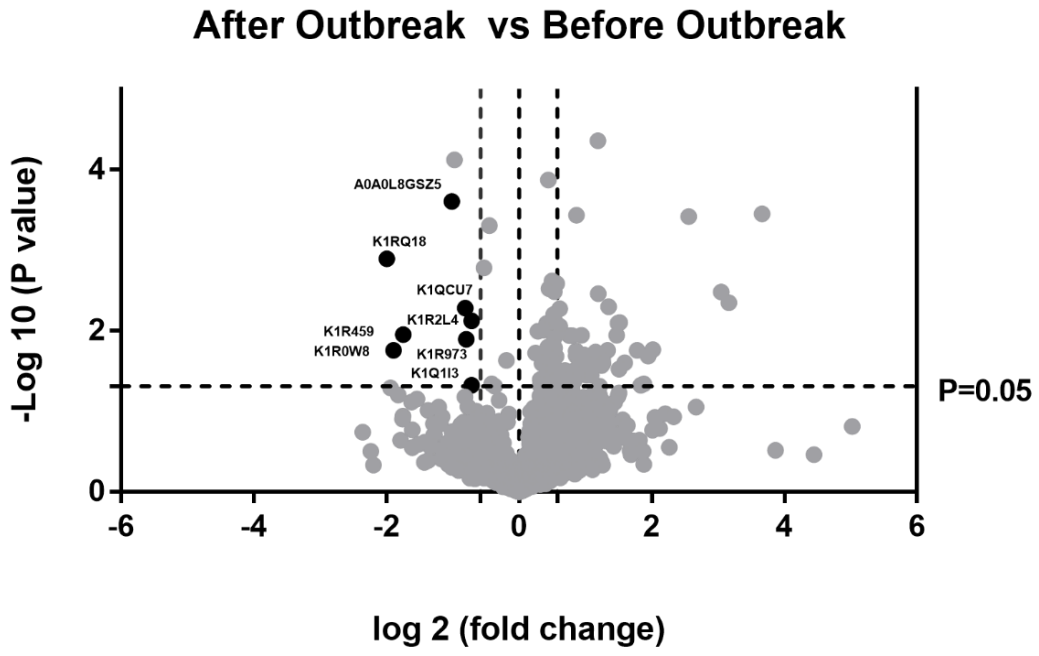

Figure 8. Graphical representation of data from quantitative proteomic analysis. Proteins are ranked in a volcano plot according to their statistical p-value and their relative abundance ratio (log2-fold change) in samples collected after and before the marteiliosis outbreak. The proteins considered as significant were those with p values < 0.05, and fold-change >1.5. Those represented by black dots and identified by their code were considered up-regulated after the outbreak.

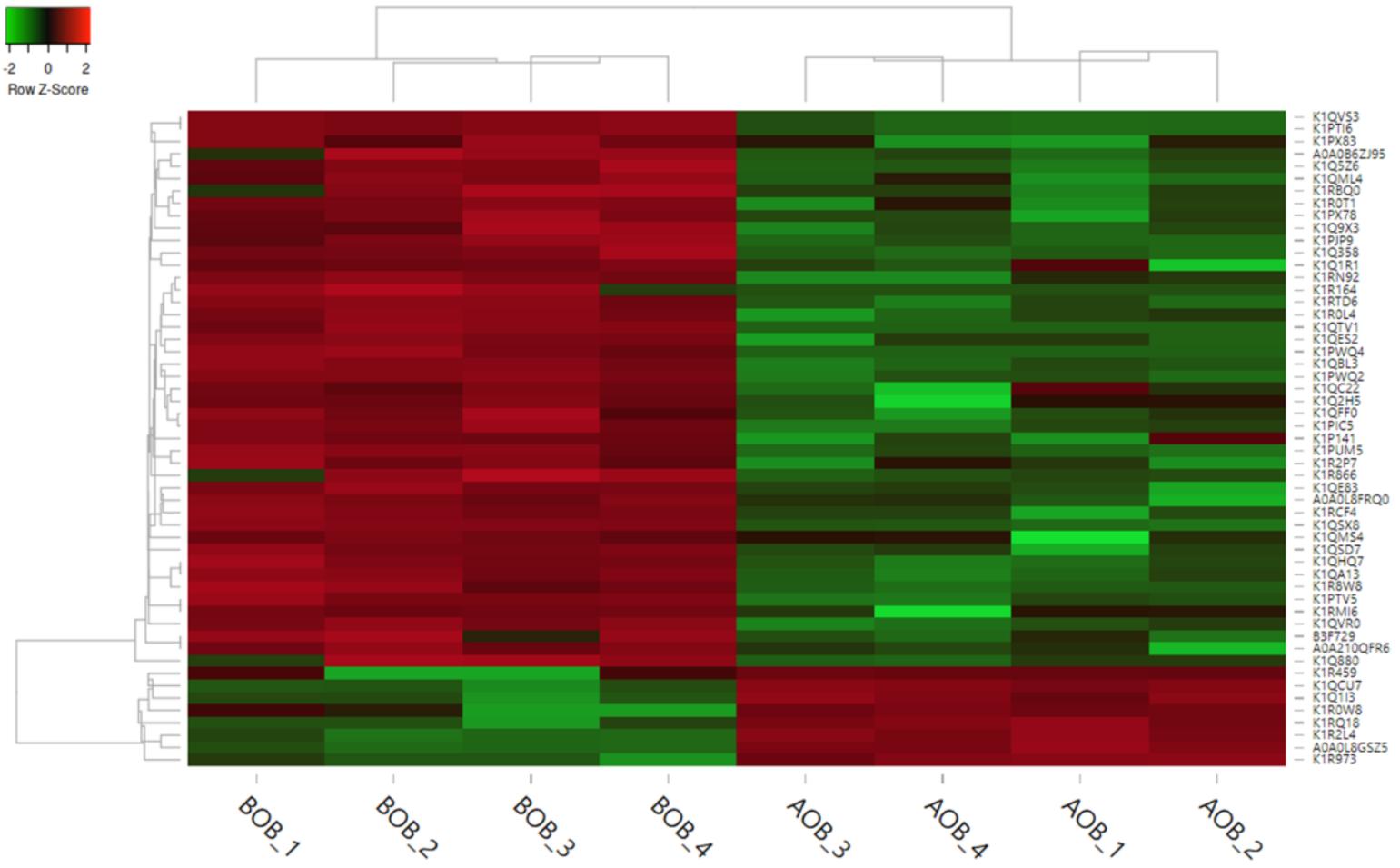

Figure 9. Cluster analysis of differentially expressed proteins. Heat map shows clustered data, each coloured cell represents a protein abundance value. The colour scale ranges from green to red, representing protein abundance from the highest level of down-regulation to the highest level of up-regulation, respectively. Protein expression values were z-score normalised prior to clustering. Columns represent different situations (AOB and BOB) while rows represent different proteins.

Considering the functional annotation of the differentially expressed proteins in the surviving cockles after the marteiliosis outbreak, the up-regulated proteins corresponded to seven protein categories in the molecular function, biological process and cellular component (Fig. 10). The categories catalytic activity, biological regulation, regulation of biological process and localization were enriched with down-regulated proteins (Fig. 10). The 45 proteins significantly down-regulated in surviving cockles are shown in Table 3. The eight proteins

significantly up-regulated in surviving cockles are shown in Table 4. Most of them have an important relationship with the immune system, which make them candidates for resistance markers.

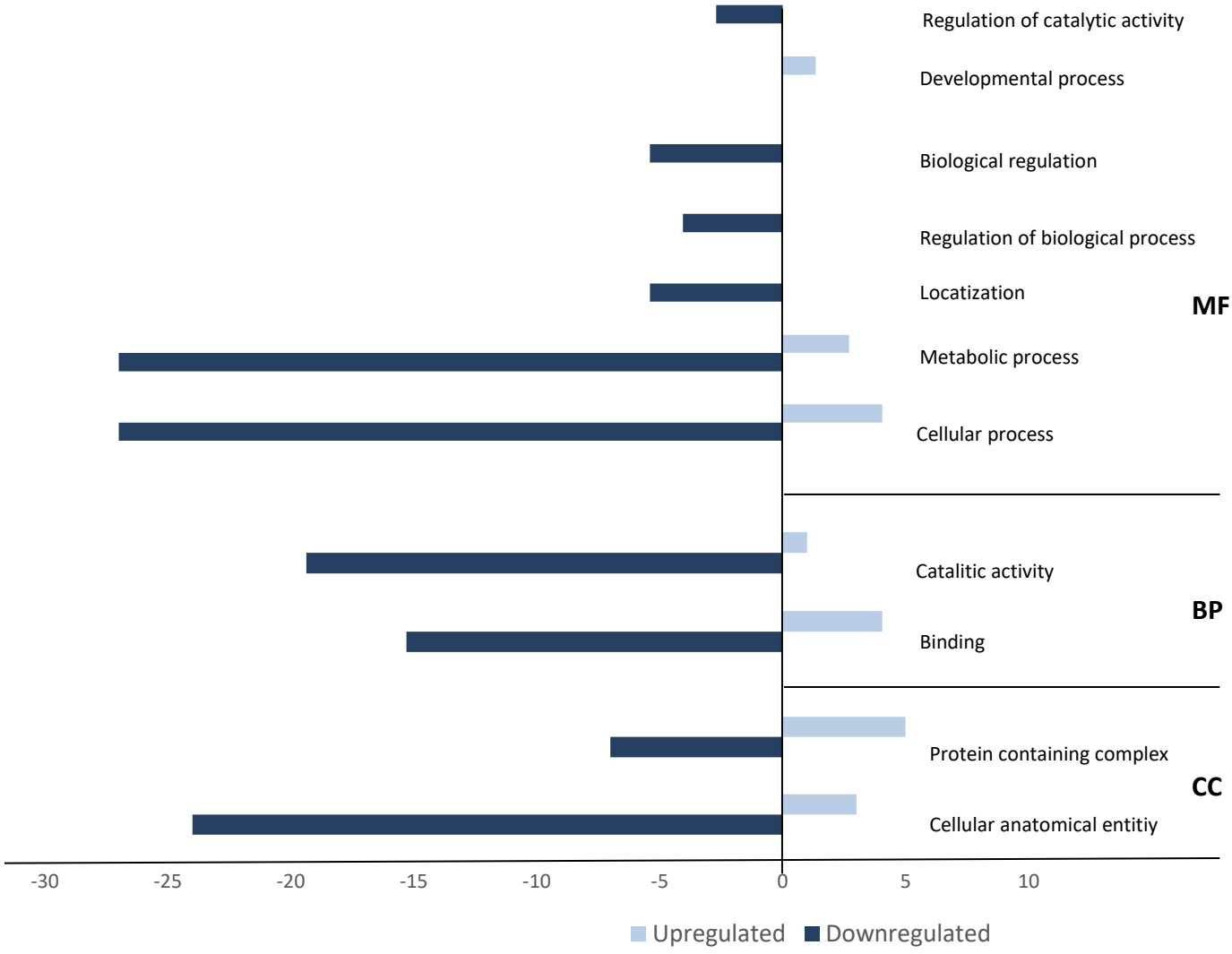

Figure 10. Gene ontology (GO) enrichment of 53 significantly regulated proteins after outbreak marteiliosis, according to the Blast 2GO functional annotation. The histogram shows for each GO term molecular function (MF), biological process (BP) and cellular component (CC) the most significantly enriched categories of up-regulated and down-regulated proteins quantified using the SWATH-MS approach.

Table 3. List of significantly down-regulated proteins in the soft tissues of cockles *Cerastoderma edule* collected after the outbreak of marteiliosis. ACCESSION: numbers (NCBI) of the homologous sequences retrieved with Blast. Fold change: measurement that describes how much an amount changes between an original and a subsequent measurement. p-value: the probability of a chance alignment occurring with a particular score or a better score in a database search.

SeqName	Description	Fold change	p-value
tr|K1PJP9|K1PJP9_CRAGI	26S proteasome non-ATPase regulatory subunit 1-like	2,816645128	0,00807277
tr|K1QVR0|K1QVR0_CRAGI	26S proteasome non-ATPase regulatory subunit 8-like	2,291543736	0,00345582
tr|K1QC22|K1QC22_CRAGI	40S ribosomal protein S19-like	1,852919865	0,03594864
tr|K1PWQ2|K1PWQ2_CRAGI	neurofilament medium polypeptide-like	1,532717241	0,00535192
tr|K1Q358|K1Q358_CRAGI	60S acidic ribosomal protein P2	1,61975338	0,03121958
tr|K1QMS4|K1QMS4_CRAGI	alpha-N-acetylglucosaminidase-like isoform X1	2,777239406	0,01135868
tr|K1PWQ4|K1PWQ4_CRAGI	asparagine synthetase [glutamine-hydrolyzing]-like	8,258312418	0,00328877
tr|K1QSX8|K1QSX8_CRAGI	trifunctional enzyme subunit alpha, mitochondrial-like	2,282945535	4,36E-05
tr|K1QA13|K1QA13_CRAGI	calcium-transporting ATPase sarcoplasmic/endoplasmic reticulum type isoform X9	1,741248073	0,01150453
tr|K1R8W8|K1R8W8_CRAGI	Hypothetical predicted protein	2,526439406	0,01757224
tr|K1RBQ0|K1RBQ0_CRAGI	caspase 7	4,050066889	0,01718315
tr|K1QE83|K1QE83_CRAGI	CCR4-NOT transcription complex subunit 1 isoform X1	1,980206328	0,01995533
tr|K1Q9X3|K1Q9X3_CRAGI	Coiled-coil domain-containing protein 81	2,318891977	0,04890038
tr|K1PUM5|K1PUM5_CRAGI	cytoplasmic aconitate hydratase-like isoform X1	1,922818884	0,01137642
tr|K1PX83|K1PX83_CRAGI	dynein heavy chain 5, axonemal-like isoform X4	3,860931226	0,02059561
tr|K1Q5Z6|K1Q5Z6_CRAGI	eukaryotic translation initiation factor 2 subunit 2-like	2,089380501	0,02691582
tr|K1Q1R1|K1Q1R1_CRAGI	exostosin-like 3	2,180448746	0,02047998
tr|K1R164|K1R164_CRAGI	galectin-4 isoform X1	3,018239959	0,02507786
tr|K1QES2|K1QES2_CRAGI	glutathione hydrolase 1 proenzyme-like	1,560076294	0,04988256
tr|K1PTI6|K1PTI6_CRAGI	glucose-6-phosphate isomerase-like	1,821691518	0,00036693
tr|K1R2P7|K1R2P7_CRAGI	hemicentin-1-like isoform X1	8,958540329	0,00449029
tr|B3F729|B3F729_CRAGI	protein Red-like	3,56956059	0,04732514
tr|K1P141|K1P141_CRAGI	keratinocyte-associated protein 2-like	2,40003284	0,02551255
tr|A0A210QFR6|A0A210QFR6_MIZYE	methylmalonyl-CoA epimerase, mitochondrial-like	2,021445444	0,03577607
tr|K1RMI6|K1RMI6_CRAGI	acyl-CoA oxidase	1,931788209	0,02296141
SeqName	**Description**	**Fold change**	**p-value**

tr|K1PTV5|K1PTV5_CRAGI	programmed cell death protein 10-like	1,801608405	0,03063665
tr|K1R866|K1R866_CRAGI	puromycin-sensitive aminopeptidase isoform X2	1,585826705	0,04917339
tr|K1QBL3|K1QBL3_CRAGI	probable phosphoglycerate mutase	1,528447034	0,00881941
tr|K1PX78|K1PX78_CRAGI	probable thiopurine S-methyltransferase	2,228039373	0,01836614
tr|K1R0L4|K1R0L4_CRAGI	sodium/potassium-transporting ATPase subunit alpha-like	1,813589992	0,02045619
tr|K1QVS3|K1QVS3_CRAGI	thimet oligopeptidase-like	5,88482195	0,00038296
tr|K1RCF4|K1RCF4_CRAGI	translocon-associated protein subunit alpha-like	2,394683837	0,02290694
tr|K1PIC5|K1PIC5_CRAGI	ER membrane protein complex subunit 4-like	2,337193938	0,02258409
tr|K1Q880|K1Q880_CRAGI	transportin-1-like isoform X1	3,684040702	0,04590246
tr|K1QSD7|K1QSD7_CRAGI	mitochondrial glutamate carrier 1-like	1,622753473	0,04108524
tr|K1RTD6|K1RTD6_CRAGI	UDP-glucose:glycoprotein glucosyltransferase 1-like	1,695430133	0,0114571
tr|A0A0B6ZJ95|A0A0B6ZJ95_9EUPU	corrinoid adenosyltransferase isoform X1	1,773080609	0,04296031
tr|K1QHQ7|K1QHQ7_CRAGI	uncharacterized protein LOC105340993	1,815884067	0,0178885
tr|K1RN92|K1RN92_CRAGI	protein PIF-like	2,37420739	0,027003
tr|K1Q2H5|K1Q2H5_CRAGI	heat shock 70 kDa protein 4-like	2,126098904	0,03562005
tr|K1QML4|K1QML4_CRAGI	isatin hydrolase	3,434899716	0,01750884
tr|K1QTV1|K1QTV1_CRAGI	CD109 antigen-like	12,68300135	0,00035214
tr|A0A0L8FRQ0|A0A0L8FRQ0_OCTBM	mitofusin-2-like isoform X2	2,547769929	0,00502208
tr|K1QFF0|K1QFF0_CRAGI	vacuolar protein sorting-associated protein 35-like	2,846870711	0,0300456
tr|K1R0T1|K1R0T1_CRAGI	V-type proton ATPase subunit G-like	2,861250396	0,00787227

Table 4. List of significantly up-regulated proteins in the soft tissues of cockles *Cerastoderma edule* collected after the outbreak of marteiliosis. ACCESSION: numbers (NCBI) of the homologous sequences retrieved with Blast. Fold change: measurement that describes how much an amount changes between an original and a subsequent measurement. p-value: the probability of a chance alignment occurring with a particular score or a better score in a database search.

Accession	Description	Fold change	p-value	Biological function
XP_034310201.1	matrilin-2-like isoform X2	3,972882792	0,00127278	Adhesion and encapsulation
XP_011439037.2	glutamate receptor 2-like	3,70741175	0,01758114	Signalling
XP_021341663.1	mucin-2-like isoform X2	3,34791146	0,01119191	Signalling
XP_029641118.1	histone H2A-like	2,015998182	0,00024726	Recognition
XP_033726259.1	vacuolar protein sorting-associated protein 13A-like isoform X6	1,752995897	0,00524303	Transport
XP_022293175.1	chloride intracellular channel protein 2-like	1,738345545	0,01276032	Signalling
XP_011427320.2	ornithine aminotransferase, mitochondrial	1,640533106	0,04732677	Metabolism
XP_034302704.1	histone H2B	1,638656964	0,00751486	Recognition

5. Conclusions

The comparison of the proteomic profiles of soft tissues from cockles collected before the marteiliosis outbreak with that from surviving cockles after the marteiliosis outbreak allowed identifying a high number of proteins representative of each condition (BOB and AOB). Furthermore, significant quantitative differences were found in the expression of 53 proteins between both conditions, from which 45 appeared down-regulated and eight up-regulated in the surviving cockles. The eight significantly up-regulated proteins in the survivors have been selected as candidate markers of resistance to marteiliosis, namely **matrilin-2-like isoform X2, glutamate receptor 2-like, mucin-2-like isoform X2, histone H2A-like, vacuolar protein sorting-associated protein 13A-like isoform X6, chloride intracellular channel protein 2-like, mitochondrial ornithine aminotransferase, and histone H2B**. The matching of these proteins with the markers of resistance to marteiliosis selected with the transcriptomic/genetic approach, within the action 7.3 of the project COCKLES, will be assessed. Additionally, these selected proteins have to be validated as true markers of marteiliosis resistance through an *ad hoc* experiment.

The results on marteiliosis dynamics showed a decrease of both marteiliosis prevalence and cumulative mortality in the cockles recruited in the inner side of the ria of Arousa compared to records of the period 2012-2016; those drops of marteiliosis prevalence and cockle mortality were likely due to an increase of resistance to marteiliosis in the cockle population of the inner side of this ria through natural selection rather than to disappearance or lower virulence of *M. cochillia*. The increase of resistance to marteiliosis through natural selection in that cockle population has to be confirmed.

6. Acknowledgements

Susana Bravo (Proteomics Service of the *Fundación Instituto de Investigaciones Sanitarias* (FIDIS), *Complejo Hospitalario Universitario de Santiago de Compostela*) provided proteomic support. M.J. Brianes Beiras, A.I. González Fontela, G. Martínez Verde, M.I. Meléndez Ramos, E. Penas Pampín, P. Rúa Santervas, P. Díaz Cedillo, J. Fernández González, I. López Maneiro, G. Pena Thomas, A. Pérez Caamaño and R. Viturro García provided technical assistance in field work and/or sample processing.

7. Literature cited

Allam, B., Raftos, D., 2015. Immune responses to infectious diseases in bivalves, Journal of Invertebrate Pathology 131: 121–136. doi: 10.1016/j.jip.2015.05.005.

Beattie, J.H., Davis, J.P., Downing, S.L., & Chew, K.K., 1988. Summer mortality of Pacific oysters. American Fishery Society, Special Publication 18: 265–268

Bonzon-Kulichenko, E., Pérez-Hernández, D., Núñez, E., Martínez-Acedo, P., Navarro, P., Trevisan-Herraz, M., Ramos, M. D. C., Sierra, S., Martínez-Martínez, S., Ruiz-Meana, M., Miró-Casas, E., García-Dorado, D., Redondo, J. M., Burgos, J. S., Vázquez, J., 2011. A robust method for quantitative high-throughput analysis of proteomes by ^{18}O labeling. Molecular & Cellular Proteomics 10: M110.003335. doi:10.1074/mcp.M110.003335.

Casas, S., Walton, W., Chaplin, G., Rikard, S., Supan, J., La Peyre, J., 2017. Performance of oysters selected for dermo resistance compared to wild oysters in northern Gulf of Mexico estuaries. Aquaculture Environment Interactions. 9: 169–180. doi: 10.3354/aei00222

Cruz, A., Da Costa, F., Fernández-Pérez, J., Nantón, A., Fernández-Boo, S., Insua, A., Méndez, J. 2020. Genetic variability in *Ruditapes decussatus* clam combined with *Perkinsus* infection level

to support founder population selection for a breeding program. PeerJ 8:e9728. doi: 10.7717/peerj.9728

de la Ballina, N.R., Villalba, A., Cao, A., 2018. Proteomic profile of *Ostrea edulis* haemolymph in response to bonamiosis and identification of candidate proteins as resistance markers. Diseases of Aquatic Organisms 128: 127-145. doi: 10.3354/dao03220

de Lorgeril, J., Petton, B., Lucasson, A., Perez, V., Stenger, P.L., Dégremont, L., Montagnani, C., Escoubas, J.M., Haffner, P., Allienne, J.F., Leroy, M., Lagarde, F., Vidal-Dupiol, J., Gueguen, Y., Mitta, G., 2020. Differential basal expression of immune genes confers *Crassostrea gigas* resistance to Pacific oyster mortality syndrome. BMC Genomics 21: 63. doi: 10.1186/s12864-020-6471-x

Dégremont, L., Garcia, C., Allen, S.K., 2015a. Genetic improvement for disease resistance in oysters: A review. Journal of Invertebrate Pathology 131: 226–241. doi: 10.1016/j.jip.2015.05.010

Dégremont, L., Nourry, M., & Maurouard, E., 2015b. Mass selection for survival and resistance to OsHV-1 infection in *Crassostrea gigas* sat in field conditions: response to selection after four generations. Aquaculture 446: 111–121. doi: 10.1016/j.aquaculture.2015.04.029

Dégremont, L., Lamy, J.-B., Pépin, J.-F., Travers, M.-A., Renault, T., 2015c. New Insight for the Genetic Evaluation of Resistance to Ostreid Herpesvirus Infection, a Worldwide Disease, in *Crassostrea gigas*. PLoS ONE 10: e0127917. doi:10.1371/journal.pone.0127917

Dégremont, L., Maurouard, E., Rabiller, M., Glize, P., 2019. Response to selection for increasing resistance to the spring mortality outbreaks in *Mytilus edulis* occurring in France since 2014. Aquaculture 511: 734269. doi: 10.1016/j.aquaculture.2019.734269

Dégremont, L., Azéma, P., Maurouard, E., Travers, M.A., 2020. Enhancing resistance to *Vibrio aestuarianus* in *Crassostrea gigas* by selection. Aquaculture 526: 735429. doi: 10.1016/j.aquaculture.2020.735429

Dove, M.C., Nell, J.A., & O'Connor, W.A., 2013. Evaluation of the progeny of the fourth-generation Sydney rock oyster *Saccostrea glomerata* (Gould, 1850) breeding lines for resistance to QX disease (*Marteilia sydneyi*) and winter mortality (*Bonamia roughleyi*). Aquaculture Research, 44: 1791-1800. doi:10.1111/are.12012

Farhat, S., Tanguy, A., Pales Espinosa, E., Guo, X., Boutet, I., Smolowitz, R., Murphy, D., Rivara, G.J., Allam, B., 2020. Identification of variants associated with hard clam, *Mercenaria mercenaria*, resistance to Quahog Parasite Unknown disease. Genomics 112:4887–4896. doi: 10.1016/j.ygeno.2020.08.036

Fernández-Boo, S., Villalba, A., Cao, A., 2016. Protein expression profiling in haemocytes and plasma of the Manila clam *Ruditapes philippinarum* in response to infection with *Perkinsus olseni*. Journal of Fish Diseases 39: 1369-1385. doi:10.1111/jfd.12470

Ford, S.E., & Haskin, H.H., 1987. Infection and mortality patterns in strains of *Crassostrea virginica* selected for resistance to the parasite *Haplosporidium nelsoni* (MSX). Journal of Parasitology, 73: 368-376. doi:10.2307/3282092

Frank-Lawale, A., Allen, S. K., Jr., & Degremont, L., 2014. Breeding and domestication of Eastern oyster (*Crassostrea virginica*) lines for culture in the mid-Atlantic, USA: line development and mass selection for disease resistance. Journal of Shellfish Research, 33: 153-165. doi:10.2983/035.033.0115

Grizel, H,, Bachere, E., Mialhe, E., Tige, G., 1987. Solving parasite-related problems in cultured molluscs. International Journal for Parasitology 17: 301–308. doi: 10.1016/0020-7519(87)90104-4

Gutierrez, A.P., Bean, T.P., Hooper, C., Stenton, C.A., Sanders, M.B., Paley, R.K., Rastas, P., Bryrom, M., Matika, O., Houston, R.D., 2018. A Genome-Wide Association Study for Host Resistance to Ostreid Herpesvirus in Pacific Oysters (*Crassostrea gigas*). Genes Genomes Genetics. 8: 1273-1280. doi: 10.1534/g3.118.200113

Gutierrez, A.P., Symonds, J., King, N., Steiner, K., Bean, T.P., Houston, R.D., 2020. Potential of genomic selection for improvement of resistance to ostreid herpesvirus in Pacific oyster (*Crassostrea gigas*). Animal Genetics, 51: 249–257. doi: 10.1111/age.12909

Hargreaves, D.C., Medzhitov, R., 2005. Innate sensors of microbial infection. Journal of Clinical Immunology 25: 503–10. doi:10.1007/s10875-005-8065-4.

Hasanuzzaman, A.F., Cao, A., Ronza, P., Fernández-Boo, S., Rubiolo, J.A., Robledo, D., Gómez-Tato, A., Álvarez-Dios, J.A., Pardo, B.G., Villalba, A., Martínez, P., 2020. New insights into the Manila clam - *Perkinsus olseni* interaction based on gene expression analysis of clam hemocytes and parasite trophozoites through in vitro challenges. *International Journal for Parasitology* 50: 195-208. doi:10.1016/j.ijpara.2019.11.008

He, Y., Yu, H., Bao, Z., Zhang, Q., & Guo, X., 2012. Mutation in promoter region of a serine protease inhibitor confers *Perkinsus marinus* resistance in the eastern oyster (*Crassostrea virginica*). Fish & Shellfish Immunology, 33: 411-417. doi: 10.1016/j.fsi.2012.05.028.

Howard, D.W., Lewi,s E.J., Keller, B.J., Smith, C.S., 2004. Histological techniques for marine bivalve molluscs and crustaceans. NOAA Tech Memo NOS NCCOS 5. US Center for Coastal Environmental Health and Biomolecular Research, Cooperative Oxford Laboratory, Oxford, MD.

Iglesias, D., Villalba, A., No, E., Darriba, S., Mariño, C., Fernández, J., Carballal, M.J., 2015. Cockle *Cerastoderma edule* marteiliosis first detected in Ria de Arousa (Galicia, Nw Spain) has spread to other Galician rias causing mass mortality. In: 17th International Conference on Diseases of fish and Shellfish, Las Palmas de Gran Canaria, Spain. Book of Abstracts, European Association of Fish Pathologists, pp. 348.

Iglesias, D., Villalba, A., Darriba, S., Cao, A., Mariño, C., Fernández, J., Carballal, M.J., 2017. Epidemiological patterns of marteiliosis affecting the common cockle *Cerastoderma edule* in Galicia (NW Spain). In: 18th International Conference on Diseases of Fish and Shellfish, Belfast, UK. Book of Abstracts, European Association of Fish Pathologists, pp. 215.

Iglesias, D., Villalba, A., Cao, A., Carballal, M.J., 2019. Is natural selection enhancing resistance against marteiliosis in cockles recruited in the inner side of the ria of Arousa? In: 18th International Conference on Diseases of Fish and Shellfish, Oporto, Portugal. Abstract Book, European Association of Fish Pathologists, pp. 184.

La Peyre, J.F., Casas, S.M., Richards, M., Xu, W., Xue, Q., 2019. Testing plasma subtilisin inhibitory activity as a selective marker for dermo resistance in eastern oysters. Diseases of Aquatic Organisms 133: 127–139. doi: 10.3354/dao03344

Lambert, J., Ivosev, G., Couzens, A. L., Larsen, B., Lin, Z., Zhong, Q., Lindquist, S., Vidal, M., Pawson, T., Bonner, R., Tate, S., & Hospital, M. S. 2014. Mapping differential interactomes by affinity purification coupled with data independent mass spectrometry acquisition. Nature Methods 10: 1239–1245. doi: 10.1038/nmeth.2702

Lapègue, S., Renault, T., 2018. Les apports de la Génétique dans la filière ostréicole Française. Bulletin de la Académie Vétérinaire de France 171:223-228. doi: 10.4267/2042/70141

Leprêtre, M., Faury, N., Segarra, A., Claverol, S., Degremont, L., Palos-Ladeiro, M., Armengaud, J., Renault, T., Morga, B., 2021. Comparative proteomics of ostreid herpesvirus 1 and Pacific oyster interactions with two families exhibiting contrasted susceptibility to viral infection. Frontiers in Immunology 11: 621994. doi: 10.3389/fimmu.2020.621994

Luo, Y., Mok, T. S., Lin, X., Zhang, W., Cui, Y., Guo, J., Chen, X., Zhang, T., & Wang, T., 2017. SWATH-based proteomics identified carbonic anhydrase 2 as a potential diagnosis biomarker for nasopharyngeal carcinoma. Scientific Reports, 7: 1–11. doi: 10.1038/srep41191

Lynch, S.A., Armitage, D.V., Coughlan, J., Mulcahy, M.F., Culloty, S.C., 2007. Investigating the possible role of benthic macroinvertebrates and zooplankton in the life cycle of the haplosporidian *Bonamia ostreae*. Experimental Parasitology 115: 359–368. doi:10.1016/j.exppara.2006.09.021

Lynch, S.A., Flannery, G., Hugh-Jones, T., Hugh-Jones, D., Culloty, S.C., 2014. Thirty-year history of Irish (Rossmore) *Ostrea edulis* selectively bred for disease resistance to *Bonamia ostreae.*

Diseases of Aquatic Organisms, 110: 113–121. doi: 10.3354/dao02734

Meistertzheim, A.L., Calvès, I., Roussel, V., Van Wormhoudt, A., Laroche, J., Huchette, S., Paillard, C. (2014). New genetic markers to identify European resistant abalone to vibriosis revealed by high−resolution melting analysis, a sensitive and fast approach. Marine Biology 161: 1883–1893. doi: 10.1007/s00227-014-2470-2

Meyer, J.G., Schilling, B., 2017. Clinical applications of quantitative proteomics using targeted and untargeted data-independent acquisition techniques. Expert Review of Proteomics 14: 419–429. doi: 10.1080/14789450.2017.1322904

Nie, Q., Yue, X., Liu, B., 2015. Development of *Vibrio* spp. infection resistance related SNP markers using multiplex SNaPshot genotyping method in the clam *Meretrix meretrix.* Fish & Shellfish Immunology 43, 469–476. doi: 10.1016/j.fsi.2015.01.030

Nikapitiya, C., McDowell, I.C., Villamil, L., Muñoz, P., Sohn, S.B., Gomez-Chiarri, M., 2014. Identification of potential general markers of disease resistance in American oysters, *Crassostrea virginica* through gene expression studies. Fish & Shellfish Immunology 41: 27–36. doi: 10.1016/j.fsi.2014.06.015

Ortea, I., Ruiz-Sánchez, I., Cañete, R., Caballero-Villarraso, J., Cañete, M.D., 2018. Identification of candidate serum biomarkers of childhood-onset growth hormone deficiency using SWATH-MS and feature selection. Journal of Proteomics, 175: 105–113. doi: 10.1016/j.jprot.2018.01.003.

Perez-Hernandez, D., Gutiérrez-Vázquez, C., Jorge, I., López-Martín, S., Ursa, A., Sánchez-Madrid, F., Vázquez, J., Yáñez-Mó, M., 2013. The intracellular interactome of tetraspanin-enriched microdomains reveals their function as sorting machineries toward exosomes. *The* Journal of Biological Chemistry, 288: 11649–11661. doi: 10.1074/jbc.M112.445304

Proestou, D.A., Sullivan, M.E., 2020. Variation in global transcriptomic response to *Perkinsus marinus* infection among eastern oyster families highlights potential mechanisms of disease resistance. Fish & Shellfish Immunology 96: 141–151. doi: 10.1016/j.fsi.2019.12.001

Proestou, D.A., Vinyard, B.T., Corbett, R.J., Piesz, J., Allen, S.K., Small, J.M., Li, C., Liu, M, DeBrosse, G., Guo, X., Rawson, P., Gómez-Chiarri, M., 2016. Performance of selectively-bred lines of eastern oyster, *Crassostrea virginica*, across eastern US estuaries. Aquaculture 464: 17–27. doi: 10.1016/j.aquaculture.2016.06.012

Ragone Calvo, L.M., Calvo, G.W., Burreson, E.M., 2003. Dual disease resistance in a selectively bred eastern oyster, *Crassostrea virginica*, strain tested in Chesapeake Bay. Aquaculture 220: 69–87. doi: 10.1016/S0044-8486(02)00399-X

Redestig, H., Fukushima, A., Stenlund, H., Moritz, T., Arita, M., Saito, K., Kusano, M., 2009.

Compensation for systematic cross-contribution improves normalization of mass spectrometry based metabolomics data. Analytical Chemistry 81: 7974–7980. doi: 10.1021/ac901143w

Shevchenko, A., Wilm, M., Vorm, O., Jensen, O. N., Podtelejnikov, A. V, Neubauer, G., Mortensen, P., Mann, M., 1996. A strategy for identifying gel-separated proteins in sequence databases by MS alone. Biochemical Society Transactions, 24: 893–896. doi: 10.1042/bst0240893

Shilov, I.V., Seymour, S.L., Patel, A.A., Loboda, A., Tang, W.H., Keating, S.P., Hunter, C.L., Nuwaysir, L.M., Schaeffer, D.A., 2007. The Paragon Algorithm, a Next Generation Search Engine That Uses Sequence Temperature Values and Feature Probabilities to Identify Peptides from Tandem Mass Spectra. Molecular & Cellular Proteomics 6: 1638–1655. doi: 10.1074/mcp.T600050-MCP200

Simonian, M., Nair, S.V., O'Connor, W.A., Raftos, D.A., 2009. Protein markers of *Marteilia sydneyi* infection in Sydney rock oysters, *Saccostrea glomerata.* Journal of Fish Diseases 32: 367−375. doi: 10.1111/j.1365-2761.2009.01022.x

Smits, M., Enez, F., Ferraresso, S., Dalla Rovere, G., Vetois, E., Auvray, J.-F., Genestout, L., Mahla, R., Arcangeli, G., Paillard, C., Haffray, P., Bargelloni, L., 2020a. Potential for Genetic Improvement of Resistance to *Perkinsus olseni* in the Manila Clam, *Ruditapes philippinarum*, Using DNA Parentage Assignment and Mass Spawning. Frontiers in Veterinary Science 7: 579840. doi: 10.3389/fvets.2020.579840

Smits, M., Artigaud, S., Bernay, B., Pichereau, V., Bargelloni, L., Paillard, C., 2020b. A proteomic study of resistance to Brown Ring disease in the Manila clam *Ruditapes philippinarum*. Fish & Shellfish Immunology 99: 641–653. doi: 10.1016/j.fsi.2020.02.002

Sunila, I., Kenyon, H, Rivara, K., Blacker, K., Getchis, T., 2016. Restocking natural beds with remote set disease resistant oysters in Connecticut: a field trial. Journal of Shellfish Research, 35: 115–125. doi: 10.2983/035.035.0113

Tan, H.T., Chung, M.C.M., 2018. Label-Free Quantitative Phosphoproteomics Reveals Regulation of Vasodilator-Stimulated Phosphoprotein upon Stathmin-1 Silencing in a Pair of Isogenic Colorectal Cancer Cell Lines. Proteomics, 18: 1–30. doi: 10.1002/pmic.201700242

Vaibhav, V., Thompson, E.L., Raftos, D.A., Haynes, P.A., 2018. Potential protein biomarkers of QX disease resistance in selectively bred Sydney Rock Oysters. Aquaculture 495: 144–152. doi: 10.1016/j.aquaculture.2018.05.035

van Banning, P., 1991. Observations on bonamiosis in the stock of the European flat oyster, *Ostrea edulis*, in the Netherlands, with special reference to the recent developments in Lake Grevelingen. Aquaculture 93: 205–211. doi: 10.1016/0044-8486(91)90232-V

Vera, M., Pardo, B.G., Cao, A., Fernández, C., Blanco, A., Gutiérrez, A., Bean, T., Houston, R.,

Villalba, A., Martínez, P., 2019. Signatures of selection for bonamiosis resistance in European flat oyster (*Ostrea edulis*): new genomic tools for breeding programs and management of natural resources. Evolutionary Applications 2019: 1781-1796. doi: 10.1111/eva.12832

Villalba, A., Iglesias, D., Ramilo, A., Darriba, S., Parada, J.M., No, E., Abollo, E., Molares, J., Carballal, M.J., 2014. Cockle Cerastoderma edule fishery collapse in the Ria de Arousa (Galicia, NW Spain) associated with the protistan parasite *Marteilia cochillia*. Diseases of Aquatic Organisms 109: 55–80. doi: 10.3354/dao02723

Wang, K., Pales Espinosa, E., Tanguy, A., Allam, B., 2016. Alterations of the immune transcriptome in resistant and susceptible hard clams (*Mercenaria mercenaria*) in response to Quahog Parasite Unknown (QPX) and temperature. Fish & Shellfish Immunology 49: 163-76. doi: 10.1016/j.fsi.2015.12.006.